IMPACT OF CLIMATE CHANGE ON THE WINTER REGIME OF THE PEACE RIVER IN ALBERTA

Alberta
Environment

IMPACT OF CLIMATE CHANGE ON THE WINTER REGIME OF THE PEACE RIVER IN ALBERTA

Prepared for:

Climate Change Research Users Group
Alberta Environment

Prepared by:

Robyn Andrishak, M.Sc. Student, E.I.T. and Faye Hicks, Ph.D., P.Eng.
Department of Civil and Environmental Engineering
University of Alberta
Edmonton, AB T6G 2G7

July 2005

Pub No. I/103
ISBN No. 0-7785-4602-0 (Printed Edition)
ISBN No. 0-7785-4603-9 (On-line Edition)
Web Site: http://environment.gov.ab.ca/info/home.asp

Disclaimer

Although prepared with funding from Alberta Environment (AENV), the contents of this report/document do not necessarily reflect the views or policies of AENV, nor does mention of trade names or commercial products constitute endorsement or recommendation for use.

Any comments, questions, or suggestions regarding the content of this document may be directed to:

Environmental Policy Branch
Alberta Environment
4th Floor, Oxbridge Place
9820 – 106th Street
Edmonton, Alberta T5K 2J6
Phone: (780) 427-6210
Fax: (780) 422-4192

Additional copies of this document may be obtained by contacting:

Information Centre
Alberta Environment
Main Floor, Oxbridge Place
9820 – 106th Street
Edmonton, Alberta T5K 2J6
Phone: (780) 427-2700
Fax: (780) 422-4086
Email: env.infocent@gov.ab.ca

SUMMARY

The effect of climate change on natural processes in the environment can be very difficult to quantify and is often of great interest to regulators and users of water resources in particular. River ice conditions along the Peace River in Alberta directly affect both the population and industries in its vicinity. As the Peace River is regulated for hydropower generation, there is a degree of human influence over the variables that determine the winter regime of the river. The purpose of this investigation was to develop a model capable of simulating thermal ice processes on northern rivers, which could, in turn, provide a means of assessing climate change effects on river ice.

The Peace River was a good case study for this research because of upstream flow regulation at the Bennett and Peace Canyon Dams in British Columbia, and the existence of a comprehensive monitoring database containing much of the data needed to run a thermal river ice model. The *River1D* thermal model was applied to the historical record for the Peace River, and results showed good agreement with water temperature measurements taken in recent years at the *town of Peace River* and *Peace River at Alces* gauge sites. The day that the zero degree isotherm reaches both locations is well represented in the simulation results, indicating that the transport and exchange of the river's heat energy is being modeled adequately. Data for the past twenty winter seasons on record (1984/85 through 2003/04) were used to assess the model's ability to simulate the progression and recession of the ice front from a downstream boundary at Fort Vermilion, Alberta (829 km downstream of the Bennett Dam). At its current stage of development, the model is considered to return reasonably accurate profiles of ice front location throughout the winter season, compared to the recorded observations.

A further objective of this project was to illustrate the potential use of the model for assessing potential climate change impacts of the thermal ice regime of regulated rivers. For this purpose, the Coupled Global Climate Model (CGCM2) "A2" climate change scenario was used to adjust the historical air temperature record and simulate corresponding ice front profiles based on conditions predicted in the year 2050. Results suggest that there is a significant potential for a reduced ice covered season under the climate change scenario investigated. Specifically, the model suggests a 33-day reduction in the duration of ice cover at the town of Peace River. In addition, the simulated maximum ice cover extent was an average of 66 km shorter after climate change, compared to the historical simulation results.

These results are, of course, preliminary at this stage as there are factors yet to consider. For example, the effects of climate change on bridging date and on the reservoir outflow temperatures need further examination. In terms of the model itself, dynamics processes such as ice cover consolidation must next be incorporated. Thus the climate change predictions should be considered qualitative indications only. Nevertheless, these results do indicate a significant potential for impact, and adaptive strategies should be considered. Models, such as the one developed here, are ideal tools for such investigations.

TABLE OF CONTENTS

SUMMARY i

LIST OF TABLES iv

LIST OF FIGURES v

LIST OF SYMBOLS viii

ACKNOWLEDGEMENTS x

1.0 INTRODUCTION 1

2.0 EQUATIONS AND MODEL DEVELOPMENT 2

2.1 Overview 2

2.1.1 Freezeup Processes 2

2.1.2 Breakup Processes 3

2.1.3 Effects of Streamflow Regulation on River Ice Processes 4

2.2 Water Cooling and Warming 5

2.3 Conservation of Water and Ice Mass 6

2.4 Ice Cover Formation 7

2.5 Ice Front Progression and Recession 11

2.6 Finite Element Implementation 11

3.0 DESCRIPTION OF STUDY REACH 15

3.1 Overview 15

3.2 Channel Geometry 15

3.3 Channel Resistance 15

4.0 PEACE RIVER ICE MODELING DATABASE 19

5.0 MODEL APPLICATION 21

5.1 Overview 21

5.2 Input Data and Parameter Set 21

5.2.1 Boundary and Initial Conditions 21

5.2.2 Atmospheric Data 22

5.2.3 Ice Modeling Parameter Set 23

5.3 Simulation of the Historical Record 23

5.3.1 Preface *23*

5.3.2 Water Temperature Profile *24*

5.3.3 Ice Front Profile *24*

5.4 Climate Change Effects on the River Ice Regime 25

5.4.1 Methodology *25*

5.4.2 Climate Change Ice Front Profile Compared to Historical Model *26*

5.4.3 Effect of Reservoir Warming Under Future Climate Conditions *26*

5.5 Discussion of Results 26

6.0 CONCLUSIONS AND RECOMMENDATIONS 33

7.0 LITERATURE CITED 35

APPENDIX A A-1

Simulated Historical Ice Front Profiles (1984/85 through 2003/04) A-1

APPENDIX B B-1

Simulated Future Climate Ice Front Profiles Compared to Historical (1984/85 through 2003/04) B-1

APPENDIX C C-1

A2 Storyline and Scenario Family C-2

References C-3

LIST OF TABLES

Table 1 Location of key sites along the Peace River 16

Table 2 Values of Mannings *n* values to be used in the model. (Source: Kellerhals, Neill and Bray, 1972) 16

Table 3 Ice modeling parameters used in preliminary model analysis 23

Table 4 Analysis of ice front profiles modeled by *River1D* compared to historical observations 27

LIST OF FIGURES

Figure 1 Generalized river cross-section with flowing surface ice 14

Figure 2 Location sketch for the Peace River study reach (adapted from Hicks, 1996) 17

Figure 3 Peace River profile used in *River1D* model (adapted from Hicks, 1996) 18

Figure 4 Peace Canyon Dam discharge (m^3/s) – winter 2003/04 20

Figure 5 Typical water temperature variation at the Peace Canyon Dam (see Section 5.2.1) 20

Figure 6 Peace River water temperature calibration at Alces gauge (2002/03) 28

Figure 7 Peace River water temperature calibration at town of Peace River (2002/03) 28

Figure 8 Water temperature validation at Alces using $h_{wa} = 15\ W/m^2/°C$ and 2003/04 freezeup data 29

Figure 9 Water temperature validation at the town of Peace River using $h_{wa} = 15\ W/m^2/°C$ and 2003/04 freezeup data 29

Figure 10 Peace River ice front profile calibration – 2002/03 30

Figure 11 Effect of reservoir warming on the simulated ice front profile using 1995/96 ice season data 30

Figure 12 Modeled historical versus future climate change date of freezeup at the town of Peace River, Alberta 31

Figure 13 Modeled historical versus future climate change date of breakup at the town of Peace River, Alberta 31

Figure 14 Modeled historical versus future climate change duration of ice cover (in days) at the town of Peace River, Alberta 32

Figure 15 Modeled historical versus future climate change minimum ice front distance (in kilometres) from the Bennett Dam in British Columbia 32

Figure A-1 Modeled and observed ice front profile – 2003/04 ..... A-2

Figure A-2 Modeled and observed ice front profile – 2002/03 ..... A-2

Figure A-3 Modeled and observed ice front profile – 2001/02 ..... A-3

Figure A-4 Modeled and observed ice front profile – 2000/01 ..... A-3

Figure A-5 Modeled and observed ice front profile – 1999/00 ..... A-4

Figure A-6 Modeled and observed ice front profile – 1998/99 ..... A-4

Figure A-7 Modeled and observed ice front profile – 1997/98 ..... A-5

Figure A-8 Modeled and observed ice front profile – 1996/97 ..... A-5

Figure A-9 Modeled and observed ice front profile – 1995/96 ..... A-6

Figure A-10 Modeled and observed ice front profile – 1994/95 ..... A-6

Figure A-11 Modeled and observed ice front profile – 1993/94 ..... A-7

Figure A-12 Modeled and observed ice front profile – 1992/93 ..... A-7

Figure A-13 Modeled and observed ice front profile – 1991/92 ..... A-8

Figure A-14 Modeled and observed ice front profile – 1990/91 ..... A-8

Figure A-15 Modeled and observed ice front profile – 1989/90 ..... A-9

Figure A-16 Modeled and observed ice front profile – 1988/89 ..... A-9

Figure A-17 Modeled and observed ice front profile – 1987/88 ..... A-10

Figure A-18 Modeled and observed ice front profile – 1986/87 ..... A-10

Figure A-19 Modeled and observed ice front profile – 1985/86 ..... A-11

Figure A-20 Modeled and observed ice front profile – 1984/85 ..... A-11

Figure B-1 Historical versus climate change modeled ice front profile – 2003/04 ..... B-2

Figure B-2 Historical versus climate change modeled ice front profile – 2002/03 ..... B-2

Figure B-3 Historical versus climate change modeled ice front profile – 2001/02 ..... B-3

Figure B-4 Historical versus climate change modeled ice front profile – 2000/01 ..... B-3

Figure B-5 Historical versus climate change modeled ice front profile – 1999/00 ..... B-4

Figure B-6 Historical versus climate change modeled ice front profile – 1998/99 ..... B-4

Figure B-7 Historical versus climate change modeled ice front profile – 1997/98 ..... B-5

Figure B-8 Historical versus climate change modeled ice front profile – 1996/97 ..... B-5

Figure B-9 Historical versus climate change modeled ice front profile – 1995/96 ..... B-6

Figure B-10 Historical versus climate change modeled ice front profile – 1994/95 ..... B-6

Figure B-11 Historical versus climate change modeled ice front profile – 1993/94 ..... B-7

Figure B-12 Historical versus climate change modeled ice front profile – 1992/93 ..... B-7

Figure B-13 Historical versus climate change modeled ice front profile – 1991/92 ..... B-8

Figure B-14 Historical versus climate change modeled ice front profile – 1990/91 ..... B-8

Figure B-15 Historical versus climate change modeled ice front profile – 1989/90 ..... B-9

Figure B-16 Historical versus climate change modeled ice front profile – 1988/89 ..... B-9

Figure B-17 Historical versus climate change modeled ice front profile – 1987/88 ..... B-10

Figure B-18 Historical versus climate change modeled ice front profile – 1986/87 ..... B-10

Figure B-19 Historical versus climate change modeled ice front profile – 1985/86 ..... B-11

Figure B-20 Historical versus climate change modeled ice front profile – 1984/85 ..... B-11

LIST OF SYMBOLS

A' --------liquid water flow area *(m^2)*

A_f -------suspended frazil ice flow area *(m^2)*

A_i --------solid ice flow area *(m^2)*

A'_f --------flow area of frazil slush at the surface *(m^2)*

$A'_{f_{new}}$ ------flow area of newly formed frazil slush at the surface *(m^2)*

B ---------top width of channel *(m)*

B_i --------surface ice width or coverage *(m)*

C_f -------suspended frazil ice concentration *(%)*

C_i --------surface ice concentration *(%)*

$C_{i_{max}}$ ------maximum surface ice concentration *(%)*

C_p -------specific heat of water *(J/kg/°C)*

e_f --------porosity of frazil slush *(dimensionless)*

H --------water surface elevation *(m)*

h_{wi} -------linear heat transfer coefficient *($W/m^2/°C$)*

K_i --------thermal conductivity of ice *(W/m/°C)*

k_{wi} -------linear heat transfer constant *(W/m^2)*

L_i --------latent heat of ice *(J/kg)*

n ---------Manning's *n* *(dimensionless)*

n_i ---------Manning's *n* for ice cover *(dimensionless)*

P_{jux} -------juxtaposition parameter *(dimensionless)*

Q' --------liquid water discharge *(m^3/s)*

Q_f -------suspended frazil ice discharge *(m^3/s)*

Q_i --------surface layer solid ice discharge *(m^3/s)*

Q'_i --------surface layer frazil slush discharge *(m^3/s)*

$Q'_{i_{new}}$ ------surface layer newly formed frazil slush discharge *(m^3/s)*

t ----------time *(s)*

T_a --------air temperature *(°C)*

t_f --------frazil (slush) thickness beneath solid surface ice *(m)*

t_f' ---------initial frazil ice thickness *(m)*

t_{f_0} --------frazil ice thickness at the beginning of a time step *(m)*

T_i ---------average ice temperature *(°C)*

t_i ---------solid thickness of surface ice *(m)*

T_m --------melting point of ice *(°C)*

T_w --------water temperature *(°C)*

U --------mean water velocity *(m/s)*

U_s --------mean surface velocity *(m/s)*

x, y, z -----coordinates for longitudinal, transverse, and vertical directions, respectively *(m)*

X_i --------location of ice front / distance from upstream boundary *(m)*

α ---------surface velocity scaling factor *(dimensionless)*

Δt --------solution time step *(s)*

η ---------frazil rise parameter *(m/s)*

ρ ---------density of water *(kg/m^3)*

ρ' --------combined density of frazil slush and pore water *(kg/m^3)*

ρ_i --------density of ice *(kg/m^3)*

ϕ_{ia} --------net rate of heat loss per unit area from ice to air *(W/m^2)*

ϕ_{iw} -------net rate of heat loss per unit area from ice to water *(W/m^2)*

ϕ_R --------net shortwave radiation reaching the water surface *(W/m^2)*

ϕ_{wa} -------net rate of heat loss per unit area from water to air *(W/m^2)*

ACKNOWLEDGEMENTS

Funding for this study was provided by the Climate Change Research User's Group (CCRUG) at Alberta Environment as well as by the Natural Sciences and Engineering Research Council of Canada (NSERC) through the MAGS (Mackenzie GEWEX Study) Research Network. This support is gratefully acknowledged. The authors would also like to thank Kim Westcott and Chandra Mahabir of Alberta Environment, for their support of this project. We truly appreciate their interest and assistance in this research. Thanks are also extended to Martin Jasek of BC Hydro for providing historical data for the study, and to BC Hydro/Glacier Power/Alberta Environment for their joint monitoring program on the Peace River which provided the detailed data for 2002/03 and 2003/04. We also thank the MAGS research group for supplying the climate change CGCM2 model results used in this study.

1.0 INTRODUCTION

An important aspect of Canadian hydrology is the influence of winter weather on streamflow behaviour, as virtually all of the rivers in Canada experience some winter ice effects each year. Throughout Alberta, increasing pressures on water quantity and quality, in response to economic development, have resulted in a need to be able to accurately quantify river discharge throughout the entire year, rather than just in the open water season. Climate change is another pressure that may add additional stress to river systems. The knowledge gained from modeling climate change scenarios contributes to a better overall awareness of river responses to various climate scenarios. In cases such as the Peace River where the flows are regulated by upstream dams, it may be possible to provide knowledge that would allow for operational adjustments of the dam to the benefit of downstream water users.

Statistical models are not valid to assess the effects of climate change on winter flows and ice regimes; only deterministic hydraulic models can achieve that. Very few hydraulic models describing ice formation and deterioration processes currently exist, and those that do exist are proprietary. To use this type of model, one must hire the developer to apply it to each individual problem, which is an impractical arrangement for Alberta Environment staff. *River1D* offers a public domain alternative. The purpose of this project was to develop the capability of assessing the impact of climate change on winter water supply in Alberta rivers. Specifically, the objective was to develop and validate a one-dimensional numerical model of Peace River flow and thermal ice processes, in order to facilitate the evaluation of the effects of meteorological conditions on the winter flow regime of this river.

Section 2.0 of this report provides details of the modeling approach used to simulate thermal river ice processes, in terms of ice growth, transport and decay. Section 3.0 presents an overview description of the characteristics of the study reach of the Peace River. Section 4.0 provides details of the extensive database collated for use as input, calibration and validation data. Section 5.0 provides details of the model application, including historic analysis (calibration and validation) and predictive analysis (for climate change scenarios). Finally, Section 6.0 presents conclusion and recommendations.

2.0 EQUATIONS AND MODEL DEVELOPMENT

2.1 Overview

An overview of river ice processes is provided in order to allow the reader to develop an understanding of the nature of the variability of ice conditions to be expected over a typical winter season. The *River1D* thermal model is based on the principles of mass, momentum, and energy conservation related to the processes described below.

2.1.1 Freezeup Processes

The onset of freezeup begins with the development of frazil particles, small discs of ice 1 to 3 millimetres (mm) in diameter, which form in supercooled water (i.e. water which is at a temperature of a few hundredths of a degree below 0°C.) In the slower flow near the banks, ice crystals develop near the surface and accumulate to form a continuous layer of skim ice on the water surface. This skim ice effectively prevents further supercooling, and subsequent ice growth is thermal in nature. The resulting ice cover is typically termed "border ice". Because ice formed by thermal heat exchange across the ice layer usually results in crystal growth in the vertical direction, a characteristic of thermal ice is its columnar crystal structure, easily recognizable in the "candles" of ice seen as this type of ice melts.

In the faster moving, turbulent flow (away from the banks), water cooled at the surface mixes into the flow and spontaneous generation of frazil particles occurs throughout the depth (again once the water temperature cools below 0°C). A small amount of heat is produced when frazil particles impinge on one another, or other objects, causing momentary melting, but refreezing is quick in the supercooled water. This results in highly adhesive behaviour of the frazil particles, causing them to accumulate, forming "frazil slush" (also known as "frazil flocs"). These frazil flocs eventually reach a size at which buoyant forces overcome the ability of the flow turbulence to maintain the flocs in suspension, and they float to the water surface. The unsubmerged portion freezes into the familiar "pancake ice" (also known as "frazil pans"). Some of the frazil particles may adhere to the bed before accumulating in sufficient quantities to float to the surface, and consequently, the frazil slush layer underlying the pans may contain sediment particles. When the frazil particles adhere to very large gravel or boulders it can remain on the bed forming "anchor ice". Some of the frazil particles or pans may also collect along the border ice. This increases the border ice encroachment on the channel, and is termed "buttering".

Frazil pans float downstream on the water surface and, as surface concentrations increase (both in time and in the downstream direction), the individual pans may freeze together forming 'rafts'. As the surface concentrations of ice floes increase to something in the order of 80 to 90%, "bridging" occurs. This involves a congestion of ice floes and a subsequent cessation of their movement along the river. Once bridging occurs, the incoming ice floes lead to an upstream progression of the ice front by 'juxtaposition' with ice floes accumulating edge to edge on the water surface. However, if flow velocities are high enough, it is also quite possible that surface ice floes coming into the ice front may be swept under the ice front and then deposited on the

underside of the cover. This process is known as "hydraulic thickening". As the ice front progresses upstream, either by juxtaposition or by hydraulic thickening, the forces acting on the ice accumulation increase. These forces include the downslope component of ice weight within the ice accumulation and the flow drag along the underside of the ice cover. These forces are resisted by the internal strength of the accumulation, which, for freezeup accumulations, is often enhanced by freezing between the individual ice floes. The forces acting on the ice cover increase as it lengthens, and when the magnitude of these forces approaches the internal strength of the ice accumulation, the ice cover is prone to collapse, or "shove", and if this happens it thickens substantially. Also the tipped pans create a significantly rougher underside surface, at least initially. The increased thickness and roughness of the ice cover after such a collapse is usually reflected in a dramatic increase in water levels. The resulting accumulation is termed a "freezeup ice jam". Normally, once the accumulation has stabilized, the water between the ice floes freezes and gives strength to the accumulation, thereby inhibiting further consolidation. In addition, frazil transport and deposition under the ice tends to smooth out the underside of the ice accumulation.

In this project, all of the thermally related ice freezeup processes will be modeled. Dynamic aspects of ice cover formation (e.g. freezeup jam development) were beyond the scope of the terms of reference.

2.1.2 Breakup Processes

The nature of breakup on a reach can vary from one in which the ice gradually deteriorates and more-or-less melts in place, to one in which breakup occurs suddenly due to the passage of a dynamic breakup front while the ice is still competent. Such dynamic fronts are generally caused by a sudden increase in streamflow runoff (for example, a combined rainfall snowmelt runoff event) or by an ice jam failure upstream.

The manner of breakup depends on a subtle trade-off between ice deterioration due to warm weather and ice cover rupture due to increased discharge. The difference in the time scales of these two processes likely explains the wide variety in the manner of breakup observed from site to site and from year to year: a rapid accumulation of heat input to the system favours a marked increase in discharge with only limited ice deterioration; a slow accumulation of heat in the system favours ice deterioration with only a limited increase in discharge. Dynamic breakup and high stages are likely in the former case; thermal breakup and only mild increases in stage are likely in the latter.

An understanding of the interaction of the flow and the ice cover are of fundamental importance to the dynamic and thermal aspects of breakup. In terms of the dynamic aspects of breakup, changes in stage and discharge cause the ice cover to lift and fall which may lead to cracking and breaking, thus releasing very competent ice to the downstream channel. Breakup ice jams typically occur under these conditions. Because temperatures are usually above freezing and cohesion effects are generally negligible, breakup ice jams would be expected to be much thicker than freezeup or winter ice jams.

Ice jam development and release is an inherently dynamic process as water goes into storage as the ice jam forms, then out of storage quite suddenly if the ice jam releases. Consequently, dramatic temporal and spatial variations in discharge can be expected during dynamic breakup events. Such dynamic processes are beyond the scope of the terms of reference of this project.

2.1.3 Effects of Streamflow Regulation on River Ice Processes

On regulated rivers, such as the Peace River, both water storage in the reservoirs and flow release patterns have the potential to significantly affect river ice processes. Reservoir storage is important because it raises winter water temperatures in the downstream reach. This occurs because of the unique density characteristics of water (Ashton, 1986). As with other fluids, water density varies with temperature. However, water density is a maximum at 4°C, and decreases with temperatures both below and above 4°C. In deep reservoirs containing water at temperatures in excess of 4°C, the cooler, denser water is found at greater depths than the warmer, less dense water. This vertical stratification is stable because further heating of the surface layers of water only leads to reduced density in these upper layers. However, as water in a reservoir cools below 4°C, it develops an inverse temperature gradient. Initially, surface heat loss lowers the water temperature in the upper layers towards 4°C, and this denser water then moves to the lower levels. As air temperatures cool the water further, water density decreases, but the colder (and less dense) water remains closer to the surface. The resulting profile is at 0°C near the surface and 4°C at the reservoir bed. Further heat loss through the winter season has the potential to cool the water through the entire depth. However, there will still be a temperature gradient until all of the water has been cooled to 0°C. This temperature gradient may persist throughout the winter in some reservoirs as the formation of an ice cover insulates the water from cold air temperatures. Snow accumulations on the ice cover enhance this insulating effect. It is important to note that the vertical temperature gradient does not persist once the water enters the river, due to the turbulent nature of the flow. Consequently, temperature measurements in the river would be expected to be homogeneous through the flow depth.

The release of warm water from a reservoir can affect a river's ice regime in three ways. First, it can inhibit the formation of an ice cover in the upper reach of the river (near the reservoir outlet). This generally leads to a prolonged and relatively unstable freezeup period (i.e. one prone to ice consolidation events). Persistence of open water in the upper reach also means that frazil production might persist through the winter period. Second, the release of warm water from a reservoir can limit the thermal growth of ice in the downstream channel. Therefore, thinner ice covers would be expected as compared to the pre-regulation period. Third, it could lead to the early melt of river ice in the spring and a greater tendency for thermal breakup events. Strategic operations during the early breakup period, specifically involving increased flow releases, can speed up the thermal deterioration of the ice cover and thus can help to minimize the possibility of dynamic breakup events.

The thermal processes, which dominate the ice regime of most regulated northern rivers, are the focus of the modeling effort here. The following sections outline the equations used to model these various thermal ice processes. They are built upon our existing one-dimensional hydrodynamic model (*River1D*), which accurately solves the equations of unsteady river flow

hydraulics. A free-drift assumption is used for the transport of frazil ice and pans; that is, surface ice is assumed to move at the surface water velocity and suspended frazil moves at the mean flow velocity.

2.2 Water Cooling and Warming

Initially, the river water temperature must cool to 0°C before any ice can be generated. Water temperature change is governed by heat exchange with the surroundings; in this case the heat balance is simplified to consider only solar heat input and linearized heat loss due to air temperature.

When there is no suspended frazil present, the change in water temperature can be modeled by the flowing equation adapted from Shen (1989):

$$\frac{\partial}{\partial t}\left(AC_p T_w\right)+\frac{\partial}{\partial x}\left(QC_p T_w\right)=-\frac{\left(B-B_i\right)\phi_{wa}}{\rho}-\underbrace{\frac{B_i\phi_{ia}}{\rho}}_{\phi_{ia}>0}-\underbrace{\frac{B_i\phi_{iw}}{\rho}}_{\phi_{iw}>0} \quad \text{.....(1)}$$

where:

A -------- cross-sectional area (see Figure 1)

$$A = BH - B_i\frac{\rho_i}{\rho}\left\{t_i+\left(1-e_f\right)t_f\right\}\ (m^2) \quad \text{.....(2)}$$

C_p ------- specific heat of water in the range [0, 20]°C (based on data from CRC, 2004)

$$C_p = 0.076\cdot T_w^2 - 3.31\cdot T_w + 4217.6\ (J/kg/°C) \quad \text{.....(3)}$$

T_w -------- water temperature *(°C)*

Q -------- water discharge

$$Q = UA\ (m^3/s) \quad \text{.....(4)}$$

ρ -------- density of water *(1,000 kg/m^3)*

ρ_i -------- density of ice *(920 kg/m^3)*

B -------- top width of channel *(m)*

B_i -------- width of ice cover *(m)*

ϕ_{wa} ------- net rate of heat transfer per unit area from water to air *(W/m^2)*

U -------- cross-section mean velocity *(m/s)*

Longitudinal dispersion is neglected.

Heat loss from water to the air is given by (Shen, 1989):

$$\phi_{wa} = h_{wa}(T_w - T_a) + k_{wa} - \phi_R \quad \text{.....(5)}$$

where:

k_{wa} ------- linear heat transfer constant *(W/m^2)*

h_{wa} ------- linear heat transfer coefficients *($W/m^2/°C$)*

T_a -------- air temperature *(°C)*

T_w ------- air temperature *(°C)*

ϕ_R -------- net shortwave radiation reaching the water surface *(W/m^2)*

Standard hydraulic computational procedures, not described here, are carried out to conserve water mass and momentum prior to ice formation. Once the water temperature reaches the freezing point, the following analysis begins to conserve water and ice mass through downstream transport.

2.3 Conservation of Water and Ice Mass

Figure 1 shows a generalized, conceptual river cross-section during the thermal freezeup process. The variables and parameters shown are defined as the relevant equations are presented. Total water mass is conserved in the pre-existing hydraulic modeling component of *River1D*. Ice mass is conserved by apportioning the water mass conservation solution from the hydraulic routine based on the mass flux between the ice and water layers.

Introduction of ice into the model begins with production of suspended frazil, quantified by volumetric concentration. Conservation of suspended frazil is given by:

$$\frac{\partial A_f}{\partial t} + \frac{\partial Q_f}{\partial x} = \frac{1}{\rho_i}\left[\underbrace{\frac{\rho}{\rho_i}\frac{(B - B_i)\phi_{wa}}{L_i}}_{\text{frazil formation if } T_w<0} - \underbrace{\rho_i \eta C_f B}_{\text{frazil rise if } C_f>0}\right] \quad \text{.....(6)}$$

where:

C_f ------- volumetric suspended frazil ice concentration *(dimensionless)*

L_i -------- latent heat of ice *(334,000 J/kg)*

e_f -------- porosity of frazil slush *(typically equal to 0.50)*

η --------- parameter representing frazil buoyancy and probability of remaining at the surface *(m/s)*

2.4 Ice Cover Formation

Once a frazil concentration is present in the flow, surface ice (pans) will begin to form and grow in thickness. Over the open water area, frazil rising to the surface creates new pans. Throughout, we assume all growth of solid ice is due to heat loss from the pan surface freezing the frazil slush beneath it. A summary of the symbols used is provided at the end of this section.

An initial frazil thickness must be assumed to start the surface ice model and to avoid $C_i \to 1$ in the first time step. The initial frazil thickness will be called t'_f and can be specified by the user. With this assumption we can convert the cross-section conservation equation for new frazil pans, given by:

$$\frac{\partial A'_{i_{new}}}{\partial t} + \frac{\partial Q'_{i_{new}}}{\partial x} = \frac{1}{\rho'}\left[\underbrace{\left(\rho_i + \rho\frac{e_f}{(1-e_f)}\right)\eta C_f (B - B_i)}_{\substack{\text{frazil and pore water deposition if} \\ C_f \geq 0}}\right] \quad \text{.....(7)}$$

$$A'_{i_{new}} = t'_f \Delta B_i \quad \text{.....(7a)}$$

$$Q'_{i_{new}} = UA'_{i_{new}} \quad \text{.....(7b)}$$

To an equation for surface ice coverage by dividing (7) by t'_f :

$$\frac{\partial B_i}{\partial t} + \frac{\partial B_i}{\partial x} = \frac{1}{\rho' t'_f}\left[\underbrace{\left(\rho_i + \rho\frac{e_f}{(1-e_f)}\right)\eta C_f (B - B_i)}_{\substack{\text{frazil and pore water deposition if} \\ C_f \geq 0}}\right] \quad \text{.....(7c)}$$

From this point on, we would build and evolve the ice thickness of existing pans using the following set of equations over the ice-covered area. The equation for frazil slush and pore water area is given by:

$$\frac{\partial A'_i}{\partial t} + \frac{\partial Q'_i}{\partial x} = \frac{1}{\rho'}\left[\underbrace{\left(\rho_i + \rho\frac{e_f}{(1-e_f)}\right)\eta C_f B}_{\substack{\text{frazil and pore water deposition if} \\ C_f \geq 0}} - \underbrace{\frac{\rho'}{\rho_i}\frac{B_i \phi_{ea}}{L_i}}_{\substack{\text{pore water freezing if} \\ \phi_{ea} > 0}} - \underbrace{\frac{\rho'}{\rho_i}\frac{B_i \phi_{es}}{L_i}}_{\substack{\text{slush melt if} \\ \phi_{es} < 0}}\right] \quad \text{.....(8)}$$

$$A'_i = t_f B_i \quad \text{.....(8a)}$$

$$Q'_i = UA'_i \quad \text{.....(8b)}$$

Solid ice area is given by:

$$\frac{\partial A_i}{\partial t} + \frac{\partial Q_i}{\partial x} = \frac{1}{\rho_i}\left[\underbrace{\frac{\rho'}{\rho_i}\frac{B_i \phi_{ta}}{L_i}}_{\substack{\text{pore water freezing if} \\ \phi_{ta} > 0}} + \underbrace{\frac{\rho}{\rho_i}\frac{B_i \phi_{ta}}{L_i}}_{\substack{\text{solid ice melt if} \\ \phi_{ta} < 0}} \right] \quad \text{.....(9)}$$

$$A_i = t_f B_i \quad \text{.....(9a)}$$

$$Q_i = UA_i \quad \text{.....(9b)}$$

If solid ice grows beyond the slush and pore water layer, equations (8) and (9) are replaced by:

$$\frac{\partial A_i}{\partial t} + \frac{\partial Q_i}{\partial x} = \frac{1}{\rho_i}\left[\underbrace{\frac{\rho}{\rho_i}\frac{B_i \phi_{ta}}{L_i}}_{\substack{\text{growth of columnar ice if} \\ \phi_{ta} > 0 \\ T_w < 0}} + \underbrace{\frac{\rho}{\rho_i}\frac{B_i \phi_{ta}}{L_i}}_{\substack{\text{solid ice melt if} \\ \phi_{ta} < 0}} - \underbrace{\frac{\rho}{\rho_i}\frac{B_i \phi_{tw}}{L_i}}_{\substack{\text{solid ice melt to warm water if} \\ \phi_{tw} > 0}} \right] \quad \text{.....(10)}$$

$$A_i = t_f B_i \quad \text{.....(10a)}$$

$$Q_i = UA_i \quad \text{.....(10b)}$$

Below is a summary of the parameters used in this section:

Direct Solution Parameters

A', Q' ---- Liquid water area (m^2) and discharge (m^3/s)

A_f, Q_f -- Suspended frazil area (m^2) and discharge (m^3/s)

$A'_{f_{new}}, Q'_{f_{new}}$ New frazil pan area (m^2) and discharge (m^3/s)

A'_f, Q'_f ---- Existing frazil pan area (m^2) and discharge (m^3/s)

A_i, Q_i ---- Solid ice area (m^2) and discharge (m^3/s)

Extractable Solution Parameters

ΔB_i ------ Change in surface ice coverage/width *(m)*

$$\Delta B_i = \frac{A'_{i_{new}}}{t'_f} \quad \text{.....(11)}$$

B_i -------- Surface ice coverage/width *(m)*

$$B_i = B_{i_o} + \Delta B_i \quad \text{.....(12)}$$

C_i -------- Surface ice concentration *(%)*

$$C_i = \frac{B_i}{B} \times 100\% \quad \text{.....(13)}$$

t_f -------- Frazil slush thickness of pans *(m)*

$$t_f = \frac{A'_i}{B_i} \quad \text{.....(14)}$$

t_i --------- Solid ice thickness of pans *(m)*

$$t_i = \frac{A_i}{B_i} \quad \text{.....(15)}$$

C_f ------- Suspended frazil concentration *(m^2/m^2)*

$$C_f = \frac{A_f}{BH - B_i \left\{ \frac{\rho_i}{\rho'} t_i + (1 - e_f) t_f \right\}} \quad \text{.....(16)}$$

Other Parameters

ρ -------- Density of water *(kg/m^3)*

ρ_i -------- Density of ice *(kg/m^3)*

ρ' ------- Combined density of frazil slush and pore water *(kg/m^3)*

$$\rho' = \rho_i (1 - e_f) + \rho e_f \quad \text{.....(17)}$$

B -------- Channel width *(m)*

B_{i_o} ------- Previous time step surface ice coverage/width *(m)*

H' ------- Water depth adjusted for ice *(m)*

$$H' = \frac{A}{B} + C_1\left[t_i\left(\frac{\rho_i}{\rho_w} - 1\right) + t_i'\left(\frac{\rho_i}{\rho_w}\left(1 - e_i^{\frac{1}{3}}\right) - 1\right)\right] \quad \text{.....(18)}$$

A -------- Total area from solution of St. Vennant Equations *(m^2)*

U -------- Flow velocity from solution of St. Vennant Equations *(m/s)*

t_i' -------- Frazil thickness of newly formed pans *(m)*

e_i -------- Frazil slush porosity

η --------- Frazil rise parameter *(m/s)*

L_i -------- Latent heat of ice *(J/kg)*

ϕ_{wa} ------- Heat loss from water to air *(W/m^2)*

$$\phi_{wa} = h_{wa}\left(T_w - T_a\right) + k_{wa} - \phi_R \quad \text{.....(19)}$$

ϕ_{ia} ------- Heat loss from ice to air *(W/m^2)* (Shen, 1989)

$$\phi_{ia} = \frac{\phi_{wa}}{\left(1 + \frac{h_{wa}t_i}{K_i}\right)} \quad \text{.....(20)}$$

ϕ_{iw} ------- Heat loss from ice to water *(W/m^2)* (Shen, 1989)

$$\phi_{iw} = \alpha_{iw}\left[\frac{U^{0.8}}{\left(H' - \frac{\rho_i}{\rho_w}\left(t_i + \left(1 - e_i^{\frac{1}{3}}\right)t_i'\right)\right)^{0.2}}\right]T_w \quad \text{.....(21)}$$

T_w -------- Water temperature *(°C)*

T_a -------- Air temperature *(°C)*

h_{wa} ------- Linear heat transfer coefficient *(W/m^2/°C)*

k_{wa} ------- Linear heat transfer constant *(W/m^2)*

ϕ_R -------- Net shortwave radiation reaching the water surface *(W/m^2)*

K_i ------- Thermal conductivity of ice – linear approximation *(W/m/°C)* (based on data from CRC, 2004)

$$K_i = 2.158 - 0.0118T_i \quad \text{.....(22)}$$

T_i -------- Ice temperature – linear approximation *(°C)*

$$T_i = \frac{T_a}{2} \quad \text{.....(23)}$$

α_{ice} Turbulent heat exchange coefficient/constant $(W \cdot s^{0.8}/m^{2.6}/°C)$

2.5 Ice Front Progression and Recession

An additional solution routine is required to specify the surface ice velocity appropriately at every node as juxtaposition of floes leads to ice cover progression. Upstream of the ice front location, the free-drift assumption applies and the surface ice velocity is directly proportional to the mean flow velocity. From the ice front downstream, the surface ice is stationary and the convective component of the surface ice equations drops out.

Locating the ice front as the numerical solution is progressing can potentially be done in a number of ways. The *River1D* thermal model is currently using the following ice front progression formula, adapted from the RICEN model (Shen *et al.*, 1995):

$$X_i(t + \Delta t) = X_i(t) - \frac{C_i U_i}{P_{ice}} \Delta t \quad \text{.....(36)}$$

This method is based on conservation of surface area of ice approaching the ice front. Bridging is initiated at the downstream boundary at a time specified by the user. There is not enough information available at this time to incorporate a bridging condition into the model itself; however, this is an ideal subject for future study.

The eventual recession of the ice cover is controlled by the model's result for surface ice thickness at the ice front location. When melt due to warm water and/or warm air reduces the total ice thickness to a small value specified in the program code (presently equal to five centimetres), the ice cover is considered "melted-out" and the ice front moves downstream to the next node.

2.6 Finite Element Implementation

The convection/conservation equations presented in the preceding sections can all be expressed in terms of the finite element method as follows. The general equation is:

$$\frac{\partial}{\partial t}(\Phi) + \frac{\partial}{\partial x}(U\Phi) = \Sigma F \quad \text{.....(25)}$$

where

Φ -------- solution parameter – combination of known values and unknown parameter

U -------- cross-section mean velocity *(m/s)*

ΣF ------ sum of all applicable flux terms

Equation (25) has the following weak statement, when using the streamline upwinded Petrov-Galerkin (SUPG) method (Hicks and Steffler, 1990):

$$\left[\int_c \left(f_i f_j + \omega \frac{L}{U} \Delta x \frac{df_i}{dx} f_j\right) dx\right] \left\{\frac{d\Phi}{dt}\right\} - \left[\int_c U \left(\frac{df_i}{dx} f_j + \omega \frac{L}{U} \Delta x \frac{df_i}{dx} \frac{df_j}{dx}\right) dx\right] \{\Phi\} + [U\Phi]_0^L = \Sigma F \quad \text{.....(26)}$$

which, on an element basis, can be further reduced to

$$\Delta x_e \begin{bmatrix} \frac{1}{3} - \frac{\omega}{2} & \frac{1}{6} - \frac{\omega}{2} \\ \frac{1}{6} + \frac{\omega}{2} & \frac{1}{3} + \frac{\omega}{2} \end{bmatrix} \frac{d}{dt} \begin{Bmatrix} \Phi_{j-1} \\ \Phi_j \end{Bmatrix} - \begin{bmatrix} U_{j-1}\left(-\frac{1}{2} + \omega\right) & U_j\left(-\frac{1}{2} - \omega\right) \\ U_{j-1}\left(\frac{1}{2} - \omega\right) & U_j\left(\frac{1}{2} + \omega\right) \end{bmatrix} \begin{Bmatrix} \Phi_{j-1} \\ \Phi_j \end{Bmatrix} = \Sigma F_j - \begin{Bmatrix} -U_0 \Phi_0 \text{, when } j-1=0 \text{ only} \\ U_L \Phi_L \text{, when } j=L \text{ only} \end{Bmatrix} \quad \text{.....(27)}$$

or, fully-assembled on a global basis, expressed as

$$[S] \frac{d}{dt} \{\Phi_j\} + [K] \{\Phi_j\} = \{F\} \quad \text{.....(28)}$$

where:

$$[S] = \sum_{e=1}^{N} [S_e] = \sum_{e=1}^{N} \begin{bmatrix} \Delta x_e \left(\frac{1}{3} - \frac{\omega}{2}\right) & \Delta x_e \left(\frac{1}{6} - \frac{\omega}{2}\right) \\ \Delta x_e \left(\frac{1}{6} + \frac{\omega}{2}\right) & \Delta x_e \left(\frac{1}{3} + \frac{\omega}{2}\right) \end{bmatrix} \quad \text{.....(29)}$$

$$[K] = -\sum_{e=1}^{N} [K_e] = \sum_{e=1}^{N} \begin{bmatrix} -U_j\left(-\frac{1}{2} + \omega\right) & -U_j\left(-\frac{1}{2} - \omega\right) \\ -U_j\left(\frac{1}{2} - \omega\right) & -U_j\left(\frac{1}{2} + \omega\right) \end{bmatrix} \quad \text{.....(30)}$$

$$\{F\} = \Sigma F_j - \begin{Bmatrix} -U_0 \Phi_0 \\ 0 \\ \vdots \\ 0 \\ U_L \Phi_L \end{Bmatrix} \quad \text{.....(31)}$$

and ω is an upwinding coefficient that is used to improve the modeling of convective processes.

Writing (28) in a time-discretized form:

$$[S]\left\{\frac{\Phi_i^{n+1}-\Phi_i^n}{\Delta t}\right\}+\theta[K]^{n+1}\{\Phi_i^{n+1}\}+(1-\theta)[K]^n\{\Phi_i^n\}=\theta\{F\}^{n+1}+(1-\theta)\{F\}^n \quad \text{.....(32)}$$

or

$$[K']\{\Phi_i^{n+1}\}=\{F'\} \quad \text{.....(33)}$$

where:

$$[K']=\left([S]+\theta\Delta t[K]^{n+1}\right) \quad \text{.....(34)}$$

$$[F']=\left([S]-(1-\theta)\Delta t[K]^n\right)\{\Phi_i^n\}+\theta\Delta t\{F\}^{n+1}+(1-\theta)\{F\}^n \quad \text{.....(35)}$$

and θ is the implicitness of the finite element method, generally taken as 0.5 (Hicks and Steffler, 1992).

From this, (10) can be solved for $\{\Phi_i^{n+1}\}$ and new nodal values of the solution parameter of interest can be extracted by dividing out the known portion of $\{\Phi_i^{n+1}\}$.

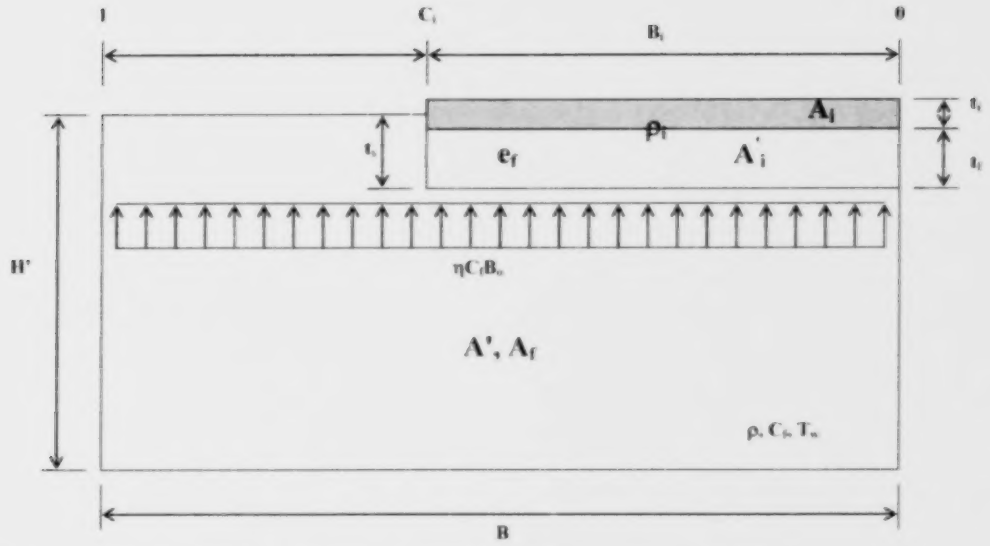

Figure 1 **Generalized river cross-section with flowing surface ice**

3.0 DESCRIPTION OF STUDY REACH

3.1 Overview

Figure 2 illustrates the study reach which extends from Hudson Hope, British Columbia (28 km downstream of the W.A.C. Bennett Dam and 5 km downstream of the Peace Canyon Dam), to Fort Vermilion, Alberta, a distance of 800 km in terms of length along the channel centerline. Blackburn and Hicks (2002) provide the following description based on information by Kellerhals *et al.*, (1972):

> *"In the upper portion of the study reach, the river is defined by a straight channel with the occasional island and mid-channel bars where the channel bed is a shallow alluvium of gravel over shale and some sandstone. Near Dunvegan the river become slightly sinuous defined by point bars and by Fort Vermilion the river displays an irregular meandering pattern characterized by a mid-channel and point bars and a channel bed consisting predominately of sand. Throughout the entire reach the river is partly entrenched and confined to the river valley."*

3.2 Channel Geometry

Hicks (1996) developed a geometric database of the Peace River using available cross section data supplemented by topographic map data. In this database, the study reach was defined using channel widths at 1 km intervals, and an effective bed profile defined as the bed elevation of an equivalent rectangular section approximating the actual channel geometry (Hicks, 1996). To define the effective bed profile, the mean bed level at each surveyed cross section was computed by first determining the hydraulic mean depth (flow area/top width) at the 1:2 year flood level and then subtracting this depth from 1:2 year flood stage. The effective bed profile was established by drawing a best-fit line through the mean bed points established from the surveyed sections. Between surveyed reaches, the water surface slope, obtained by identifying locations where topographic contours intersected the river channel on 1:250,000 scale National Topographic Series (NTS) maps, was used to estimate the gradient of the effective bed profile. Surveyed water level profiles by the Alberta Research Council and Environment Canada were also used to refine the profile (e.g. to define the Vermilion Chutes downstream of Fort Vermilion). The input channel widths were based on channel top widths measured from the 1:250,000 NTS maps. The resulting geometric database consists of more than 1100 computational nodes spaced at 1 km intervals. Table 1 provides the locations of key sites along the river, while Figure 3 illustrates the bed profile used in the model.

3.3 Channel Resistance

Channel resistance in the model can be input in terms of Manning's n or roughness height, k. For the present study, Manning's n will be used as data were readily available, since it is the more common for such applications. Table 2 presents the values to be used in the various sub-reaches of the Peace River. These were estimated based on the values presented by Kellerhals *et al.*

(1972). Hicks and McKay (1995) conducted hydraulic simulations of all open water seasons dating back to 1972, confirming the applicability of these channel resistance values.

Table 1 Location of key sites along the Peace River

Location	Station (km downstream of the Bennett Dam)
Peace Canyon Dam	23
Peace River at Hudson Hope	28
Halfway River confluence	65
Moberly River confluence	103
Peace River at Fort St. John	110
Pine River confluence	120
Peace River at Taylor	121
Beaton River confluence	141
Kiskatinaw River confluence	154
Peace River at Alces gauge	164
British Columbia-Alberta border	166
Clear River confluence	186
Peace River at Dunvegan Bridge	295
Smoky River confluence	388
Heart River confluence	394
Peace River at Peace River	395
Notikewin River confluence	558
Peace River near Carcajou	650
Peace River at Fort Vermilion	808
Boyer River confluence	819
Wabasca River confluence	865
Peace River at Peace Point	1107

Table 2 Values of Mannings *n* values to be used in the model. (Source: Kellerhals, Neill and Bray, 1972)

Location (km)	Manning's *n*
28 to 75	0.030
75 to 210	0.045
210 to 345	0.025
345 to 1107	0.020

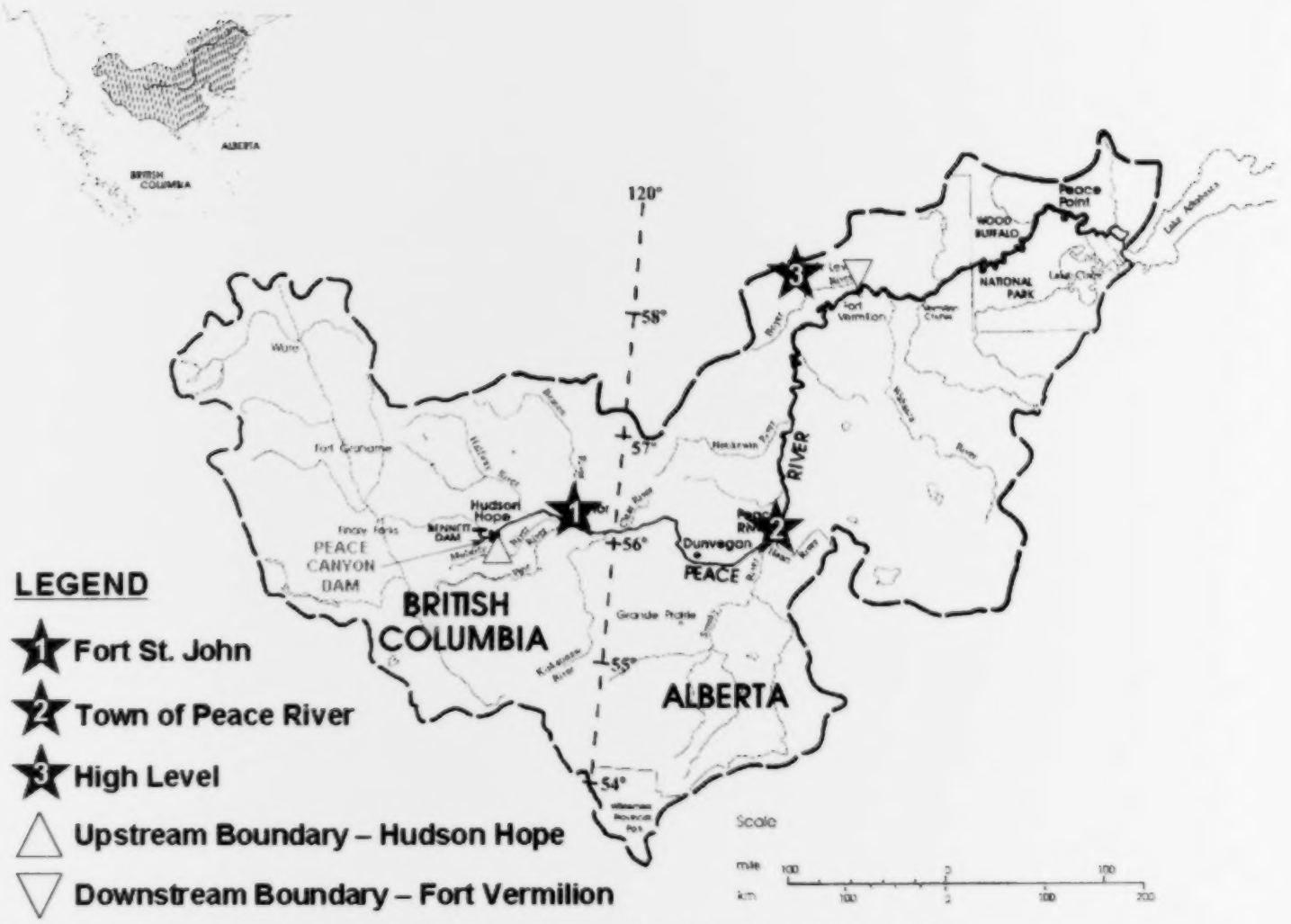

Figure 2 **Location sketch for the Peace River study reach (adapted from Hicks, 1996)**

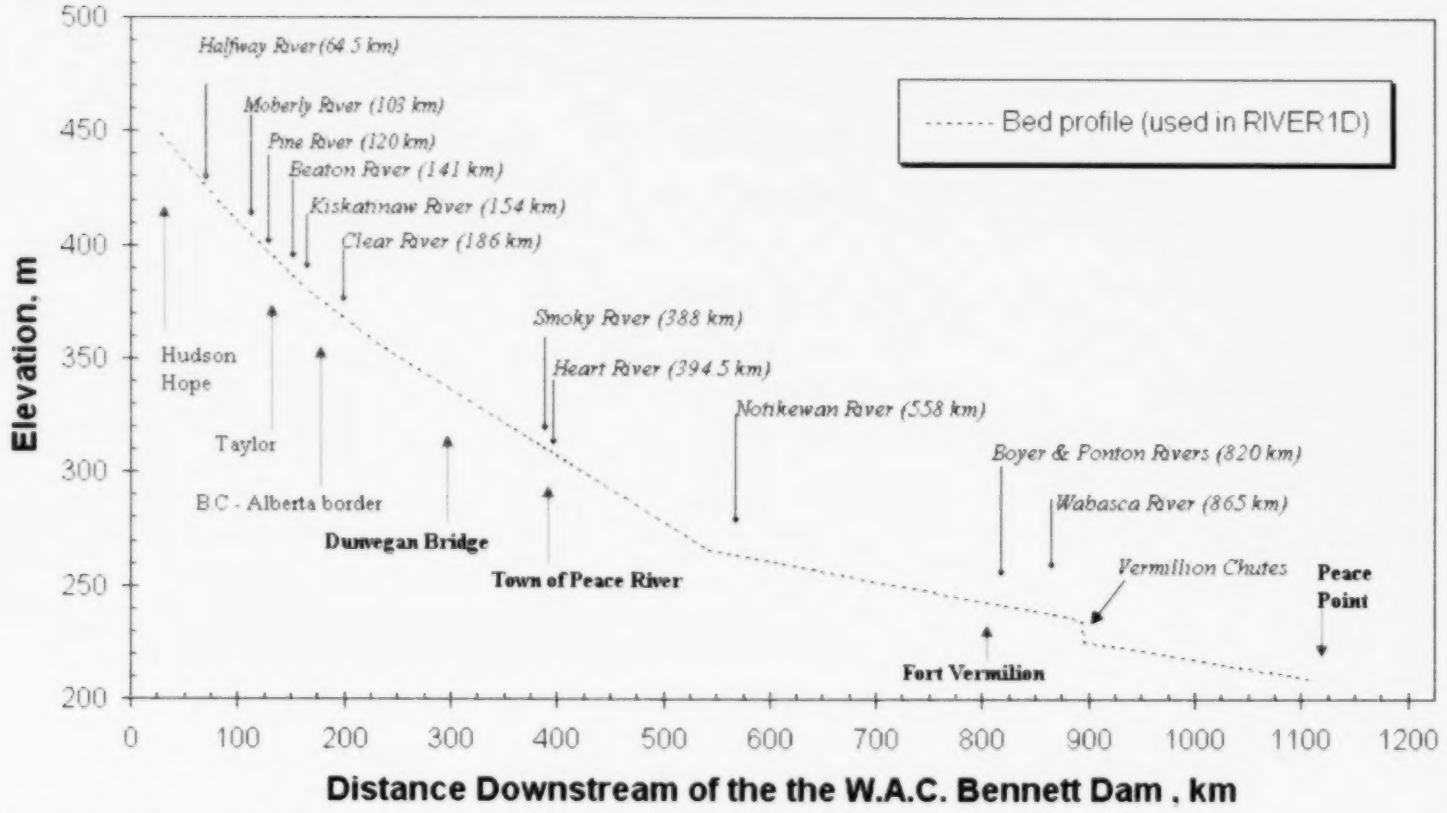

Figure 3 **Peace River profile used in *River1D* model (adapted from Hicks, 1996)**

4.0 PEACE RIVER ICE MODELING DATABASE

Alberta Environment, B.C. Hydro, and their collaborators have been collecting winter data on the Peace River for several years. The most comprehensive and complete data collected, including water temperature, ice concentration, and solar radiation are available for the 2002/03 and 2003/04 ice seasons. All relevant historical data have been collected and assembled in an ice modeling database for the Peace River. This database is available from the authors on CD-ROM.

The primary information needed to run the thermal *River1D* model are the upstream boundary discharge and water temperature, as well as the air temperature over the basin. Since the winter discharge of the Peace River is controlled by the WAC Bennett and Peace Canyon hydropower dams in northwestern British Columbia, and demand for power typically peaks in the cold winter months, the winter discharge much higher than the unregulated winter flow would otherwise be. Figure 4 illustrates the flow variation for the winter of 2003/04.

The tailrace water temperature at the upstream end of the Peace River follows a relatively regular annual variation. The "typical" discharge water temperature profile is shown in Figure 5. This temperature profile will be discussed further in Section 5.2.1.

The air temperature records at various locations throughout the Peace River basin are the most complete and lengthy of the thermal data available. The model allows for the basin to be split up into air temperature zones that correspond to a chosen air temperature monitoring station. However, where there is a reasonable correlation between stations in the basin, an average air temperature can be used over a larger area.

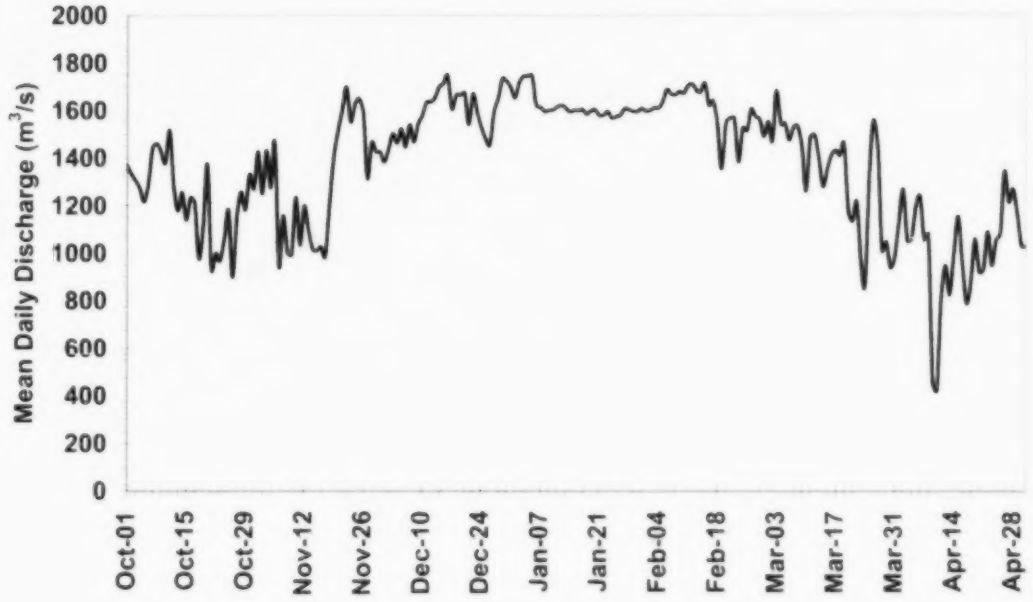

Figure 4 **Peace Canyon Dam discharge (m^3/s) – winter 2003/04**

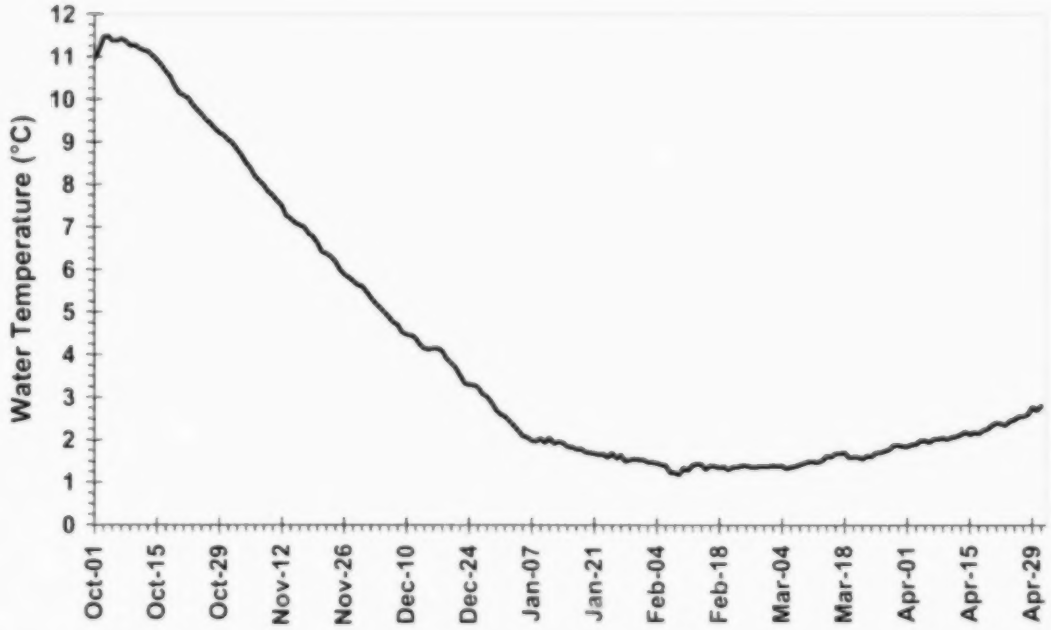

Figure 5 **Typical water temperature variation at the Peace Canyon Dam (see Section 5.2.1)**

5.0 MODEL APPLICATION

5.1 Overview

A key objective of this study is to illustrate *River1D*'s ability to predict the potential impacts of climate change on the ice regime of Alberta rivers by demonstrating it on the Peace River. Model application involved two key steps. First, various river ice process parameters (discussed in Section 2.0) were calibrated, and the resulting ice process model validated. The historical record provided the data for this effort. Second, the model was used in a predictive sense, to explore the potential impacts of climate change scenarios on the future ice regime of the Peace River.

The model evaluation had to be limited to the period after construction of the Peace Canyon Dam (i.e. after 1982), since its impoundment of water affects the thermal ice regime of the Peace River. For this preliminary evaluation of the *River1D* thermal river ice model, the past 20 ice seasons on record (1984/85 through 2003/04) were considered adequate to assess the model's capabilities providing a substantial range of winter conditions.

The upstream boundary for all model runs had to be taken downstream of the Peace Canyon Dam, again due to its influence on the thermal regime of the Peace River. For convenience, the upstream boundary of the model was actually taken 5 km further downstream, at the WSC gauge at Hudson Hope, BC, as this was the upstream boundary of the earlier hydraulic model developed and validated by Hicks (1996). Later sensitivity analyses indicated that this was sufficiently close to the Peace Canyon Dam to also be a valid choice from a thermal modeling perspective. In terms of stationing, this upstream boundary is located at km 28 (referenced in terms of distance downstream of the WAC Bennett Dam, simply for consistency with previous hydraulic studies). The downstream boundary for this study was set near Fort Vermilion, AB, specifically at km 829, since this is where bridging typically occurs during freeze-up.

Ice season simulations were generally run from noon November 1 to noon May 1. Years in which the ice front initiated in the second or third week of November were modeled from October 15 to ensure that the upstream initial water temperature had enough time to travel the entire 800 km reach modeled prior to downstream bridging. This ensured that the assumed initial conditions within the modeled reach had no effect (positive or negative) on the simulated ice front progression. Years for which modeling from mid-October was necessary were: 1996/97, 1995/96, 1989/90, 1986/87, 1985/86, and 1984/85.

5.2 Input Data and Parameter Set

5.2.1 Boundary and Initial Conditions

Time series for inflow discharge, water temperature, suspended frazil ice concentration, surface ice concentration, surface frazil ice thickness, and solid ice thickness are the physical boundary conditions required to run the *River1D* thermal river ice model. In addition to these upstream boundary conditions, a downstream rating curve, water level, or outflow discharge time series must be specified to satisfy the requirements of the hydraulic modeling component. Initial

conditions for discharge, water level, water temperature, suspended frazil ice concentration, surface ice concentration, surface frazil ice thickness, and solid ice thickness are required for every specified node to initiate the model simulation. Downstream boundary conditions for the thermal modeling variables above (water temperature, ice thicknesses, etc.) are not required as the finite element scheme in *River1D* employs natural boundary conditions to compute these variables.

To construct the boundary condition time series, mean daily values from the available record were specified at 24-hour time intervals, ranging from the simulation start time to several days beyond the anticipated simulation end time. It may be important to note that the model operates on a much smaller time step and could actually take advantage of more detailed input data. However, this is likely more of interest to operational applications of the model, and thus this particular input data limitation was not considered critical for the purposes of the current study.

The first discharge and water temperature in the boundary time series was used as the initial condition for these variables at every node. The initial water level profile was determined by running a hydraulic computation with *River1D* until the solution achieved a steady-state. The discharge record for the Peace Canyon Dam was used to specify the inflow time series. This information, obtained from Alberta Environment, is extensive and complete for all of the years modeled. No substitution for missing data was required for the analysis.

The Peace Canyon Dam tailrace water temperature record was used to build the upstream boundary time series. The quality and completeness of these data were well below that of the discharge record. No record is available for ice seasons during the years 1984 through 1988, nor for 1998. Analysis of the historical data revealed a relatively consistent water temperature profile (Figure 5). The "typical" water temperature profile was obtained by averaging 9 years on record with corresponding daily values within a range of ±1°C of each other. The years used to calculate this temperature trend are: 1980/81, 1982/83, 1990/91, 1991/92, 1994/95, and 2000/01 through 2003/04. This mean profile was used as the upstream boundary condition where measured data was unavailable.

Ice conditions at the upstream boundary were all held at zero for the duration of simulations, consistent with tailrace conditions expected from the Peace Canyon Dam. This can be realistically assumed because water issuing from the dam is consistently above 0°C throughout the winter, thus no ice forms at this upstream boundary of the modeled domain.

5.2.2 Atmospheric Data

In the present model, air temperature determines the energy exchange between the river and the atmosphere. *River1D* is also able to use solar radiation data in its heat transfer model; however, neither an adequate spatial nor temporal dataset is available at this time to take advantage of this feature.

For this study, the Peace River reach being modeled was split into two atmospheric zones. The southern zone, extending from the upstream boundary to km 400 km used the average of air temperature measurements on record at Fort St. John, BC, the town of Peace River, AB, and the

WSC gauge at Alces (where available). The northern zone, downstream of km 400 to Fort Vermilion, AB, used the air temperature record from High Level, Alberta.

The air temperature records at Fort St. John, the town of Peace River, and High Level cover all the years considered in this study, thus no substitution for missing air temperature data was required. Air temperature data at the WSC gauge at Alces is available from January 1994 to present; it was used to further refine the atmospheric conditions over the southern zone during the 1994/95 through 2003/04 seasons.

5.2.3 Ice Modeling Parameter Set

There are several physical parameters related to the ice modeling processes handled by *River1D*. The values used for this study are based on the authors' opinion of reasonable values and work being done by their collaborators. Table 3 provides a list of the ice modeling parameters and the values used for this analysis.

Table 3 Ice modeling parameters used in preliminary model analysis

Parameter (units)	Value
e_f, porosity of frazil slush *(dimensionless)*	0.5
η, frazil rise parameter *(m/s)*	0.0001
n_i, Manning's *n* for ice cover *(dimensionless)*	0.02
$C_{i_{max}}$, maximum surface ice concentration *(%)*	100
α_{tw}, turbulent heat exchange coefficient *($W{\cdot}s^{0.8}/m^{2.6}/°C$)*	1187
P_{jux}, juxtaposition parameter *(dimensionless)*	2.5

In addition, the time of ice front initiation (bridging) must be specified. For this study, the ice front observations provided by Alberta Environment were used either directly to determine the date of bridging at Fort Vermilion or, for years when the first observation was upstream of the downstream boundary, the observations were extrapolated to estimate a value. Where the bridging time was estimated in this way, it became a calibration parameter and was adjusted forward or backward to best match the simulated ice front profile.

5.3 Simulation of the Historical Record

5.3.1 Preface

It is stressed that the hydraulic component of the model has already been extensively validated (Hicks and McKay, 1995, Hicks, 1996, Blackburn and Hicks, 2002); thus this effort focuses upon the calibration and validation of the thermal ice modeling components only.

5.3.2 *Water Temperature Profile*

The first component of the model to be evaluated is the water temperature. Reliable water temperature modeling is critical to the accuracy of any subsequent ice modeling effort, as this determines when and where ice generation occurs.

Water temperature observations on the Peace River in Alberta are currently limited to two locations: the WSC gauges at Alces River (km 296 km) and the town of Peace River. The records at these locations date back to March 2002 and September 2001, respectively. It is also noted that the water temperature probes used at these sites are subject to offset and measurement error. For this analysis, the minimum water temperature recorded during the winter months was shifted to 0°C to eliminate measurement offset.

The heat transfer coefficient, h_{wa}, was the only parameter used to calibrate the model for this study. The heat transfer constant, k_{wa}, and solar radiation were kept at zero. The values of h_{wa} tested are based on the preliminary results of the work done for earlier studies on the Peace River (eg. Andres, 1993).

The 2002/03 season was used to calibrate the water temperature model output. Figure 6 and Figure 7 show the observed and modeled water temperature profiles at the WSC gauge sites at Alces and at the town of Peace River. The most important criterion in evaluating these results is in terms of how well the presence of 0°C water (or the arrival of a zero-degree isotherm) is simulated compared to the observations, as this determines whether or not the model will generate ice in the right places at the right times. On this basis, the simulations corresponding to h_{wa} = 15 $W/m^2/°C$ appear to perform better than those for h_{wa} = 10 $W/m^2/°C$ and h_{wa} = 20 $W/m^2/°C$, particularly at the town of Peace River. Therefore, a value of h_{wa} = 15 $W/m^2/°C$ was adopted for the reach upstream of the town of Peace River. Initially this value was applied to the entire study reach; however, upon initial calibration of the simulated ice front profiles (see Section 5.3.3), a value of h_{wa} = 10 $W/m^2/°C$ was deemed more appropriate for the northern reach of the river (downstream of the town of Peace River) to address simulated production of ice that considerably exceeded the observed data. Water temperature data north of the town of Peace River would be helpful for further calibration and validation of these heat transfer coefficient selections, but such data is not available at this time.

Validation of the heat exchange component of the *River1D* model for the Peace River was done using data from the 2003/04 season. The water temperature profiles for this run are shown in Figure 8 and Figure 9. These results show good agreement with the observed water temperatures at Alces and the town of Peace River. Most significantly, the model is able to match the day the zero degree isotherm reaches these two observation stations reasonably well.

5.3.3 *Ice Front Profile*

Twenty years of ice front observations on the Peace River, 1984/85 through 2003/04, were used to evaluate the ice modeling components of *River1D*. The 2002/03 season, shown in Figure 10, served as the calibration base year. A series of juxtaposition parameter (P_{jux}) values from 1.5 to 3.0 were tested. In terms of the best representation of the simulated approach of the ice cover

towards, and date of freezeup at, the town of Peace River, $P_{flux} = 2.5$ was considered the most reasonable value.

The complete set of modeled and observed ice front profiles using the aforementioned calibration of h_{wa} and P_{flux} can be found in Appendix A. Considering the complete collection of historical runs performed, the *River1D* thermal river ice process model produces a reasonable ice front profile in the majority of these years. In general, the maximum extent of ice cover is greater than the observations recorded. However, considering the fact that the model does not include dynamic surface ice processes and secondary consolidation, this result is not unexpected as these processes are known to occur on the Peace River. Seasons such as 1995/96 are extremely well modeled by *River1D*, suggesting that simple juxtaposition of floes may have been the dominant process taking place that year.

These model results validate *River1D*'s ability to predict the general trend of ice front location on the Peace River, despite the effect of dynamic processes not currently handled by the model.

5.4 Climate Change Effects on the River Ice Regime

5.4.1 Methodology

Canadian Centre for Climate Modelling and Analysis (CCCma) Coupled Global Climate Model (CGCM2) output was selected for this assessment of the impact of climate change on the Peace River as two standardized future climate scenarios were available from the Mackenzie GEWEX Study (MAGS) research group: A2 and B2. The A2 scenario (described in more detail in Appendix C) is based upon projections of larger population growth and higher cumulative carbon dioxide (CO_2) emissions over the period 1990 to 2100, as compared to the B2 scenario. As a result, the magnitude of climate warming under the A2 scenario is the more severe of the two, which is the primary reason it was selected for this analysis. Each scenario contains three future projections for air temperature and precipitation changes over the baseline: specifically for 2010, 2050, and 2080. The baseline is taken as the thirty-year period 1961-1990. For this initial research, the projection to the year 2050 was chosen as a balance between the "too near" and "too far" projections.

To determine future air temperatures at a given location, the baseline historical record is shifted by the change value given by the CGCM2 model for the corresponding location. The climate model predictions are given in the form of mean monthly values, so the actual future climate predictions are limited to these means. For example, if the average January air temperature for the town of Peace River during the 1961-1990 period was -17.1°C and the CGCM2 air temperature change value for January 2050 in the Peace River area is +5.7°C, we can predict that the average January air temperature in 2050 would be -11.4°C.

Monthly average air temperatures are not sufficient to model river ice processes or conduct a detailed analysis of future ice conditions on the Peace River. In order to assess the effects of climate change on the winter ice regime, we have assumed that the mean daily air temperature readings from 1984/85 through 2003/04 can be shifted by the climate change values for corresponding months to obtain a future air temperature time series.

5.4.2 *Climate Change Ice Front Profile Compared to Historical Model*

All twenty historical years were re-run with their air temperature time series adjusted based on the change values for the year 2050 obtained from the CGCM2 A2 climate scenario. All other input data, parameters, and constants remained the same. The complete set of future climate ice front profiles compared to the simulated historical ice front model profiles can be found in Appendix B. It should be noted that climate change is also likely to impact the date of initial bridging, an issue which was beyond the scope of the present study. Unfortunately, current knowledge of the bridging process does not allow us to quantify the impact of climate change on this aspect of the ice regime. Thus, for this preliminary climate change evaluation, the date of bridging was not adjusted in any way.

5.4.3 *Effect of Reservoir Warming Under Future Climate Conditions*

It is quite possible that climate warming could elevate the reservoir water temperature in the Bennett and/or Peace Canyon Dam reservoirs, shifting the typical discharge water temperature profile (Figure 5) upward. Although assessing the impact of climate change on large reservoirs is a complex task that was beyond the scope of this particular study, the importance of this issue was evaluated in a general sense by employing a sensitivity analysis. Specifically, the 1995/96 simulation was repeated with the inflow water temperature time series at the upstream boundary increased uniformly by 0.5°C and 1.0°C, values considered within the realm of possibility based on intuitive judgment.

Figure 11 shows the results of the reservoir water temperature sensitivity analysis. As might be expected, the increasing water temperatures at the headwaters of the Peace River resulted in an upward shift of the ice front profile. However, this change appears to have little effect on the early winter freezeup conditions. The effect of warmer water temperatures is more apparent in the late winter and during spring melt.

5.5 Discussion of Results

Considering the assumptions and level of sophistication of the model at its current stage of development, the model performs reasonably well in most of the historical seasons tested. Table 4 provides some statistics on the key parameters arising from the modeled ice front profiles. This analysis shows that the model is able to simulate the date of freezeup, breakup, and duration of ice cover at the town of Peace River with a good degree of overall accuracy. The maximum extent of ice cover is not currently as well modeled, as is apparent from the statistics shown in the same table.

Warmer air temperatures consistent with climate change can be expected to result in later freezeup, earlier breakup, fewer ice covered days, and reduced extent of ice on the Peace River. The as yet un-quantifiable effect of climate change in delaying the date of initial ice cover formation (i.e. bridging) at Fort Vermilion could further reduce the duration and extent of the ice cover on the Peace River.

Until a suitable, deterministic bridging criterion or model can be defined for the Peace River, the present climate change analysis is limited to the assumption of no change in bridging date, and thus the future climate comparisons that follow should be considered conservative. Figure 12 shows the trend towards later freezeup at the town of Peace River under the future climate scenario considered. Figure 13 illustrates the consistent modeled trend towards earlier future breakup at the same location. There is somewhat greater consistency in the breakup results than the freezeup results, which could perhaps be attributed to neglecting the effect of climate change on delaying bridging.

Table 4 Analysis of ice front profiles modeled by *River1D* compared to historical observations

Ice front parameter	Average	Absolute Maximum	Absolute Minimum	Std. Dev.
Error in modeled date of freezeup at the town of Peace River (in days)	-2.5	51	1	15.3
Error in modeled date of breakup at the town of Peace River (in days)	-1.2	20	0	7.8
Error in modeled duration of ice cover at the town of Peace River (in days)	1.5	55	0	19.6
Error in modeled extent of ice cover (minimum distance from Bennett Dam in kilometers)	57	122	5	41

Figure 14 also shows a relatively consistent reduction in the duration of ice cover at the town of Peace River. Finally, Figure 15 illustrates the change in maximum extent of ice cover on the Peace River. The slope of the regression line in this figure deviates much more from the 1:1 line than in the other three figures and the coefficient of determination for ice cover extent is the highest. This would tend to suggest that the effect of climate change on the persistence of open water throughout the winter will be most significant in milder years corresponding to those in which the ice cover peaked historically farther downstream of the dam. In contrast, colder than average years would then exhibit less dramatic changes in maximum ice cover extent under analogous future climate conditions.

Based on the current model and analysis, the freezeup date is projected to be, on average, 16 days later and the breakup date almost 17 days earlier at the town of Peace River by the middle of the century. This amounts to an overall reduction in the duration of ice of 33 days. Finally, the modeled maximum extent of ice is reduced by an average of 66 kilometres under the future climate change scenario.

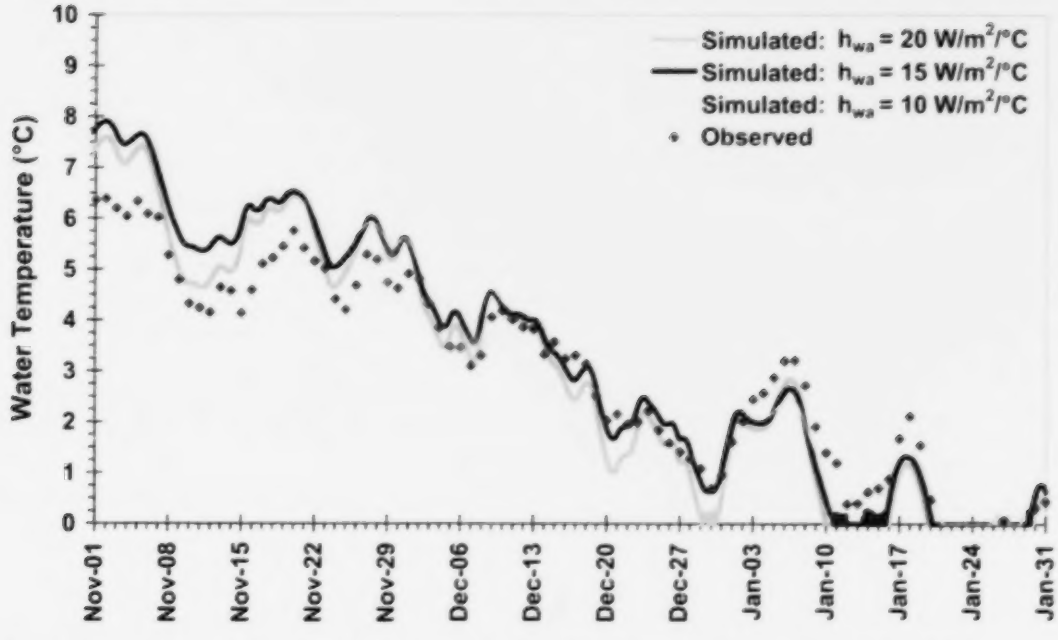

Figure 6 **Peace River water temperature calibration at Alces gauge (2002/03)**

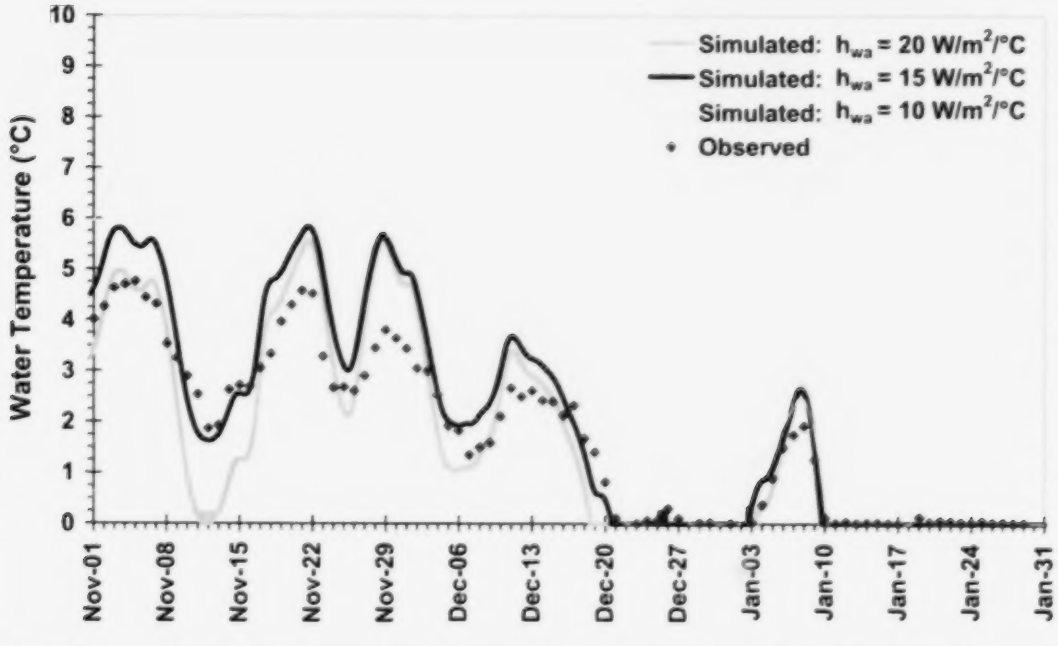

Figure 7 **Peace River water temperature calibration at town of Peace River (2002/03)**

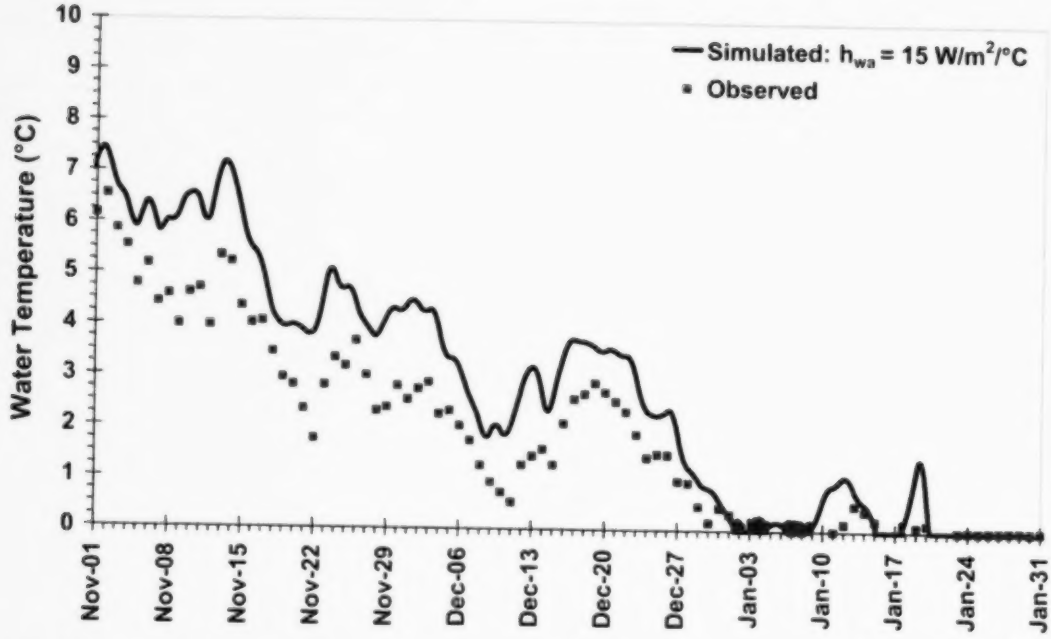

Figure 8 Water temperature validation at Alces using h_{wa} = 15 $W/m^2/°C$ and 2003/04 freezeup data

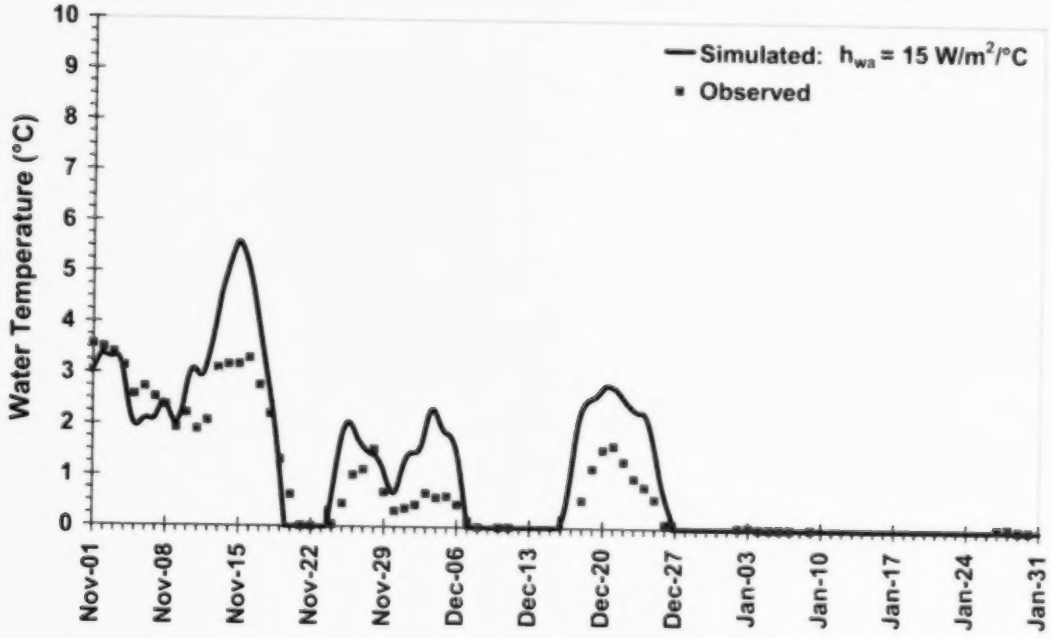

Figure 9 Water temperature validation at the town of Peace River using h_{wa} = 15 $W/m^2/°C$ and 2003/04 freezeup data

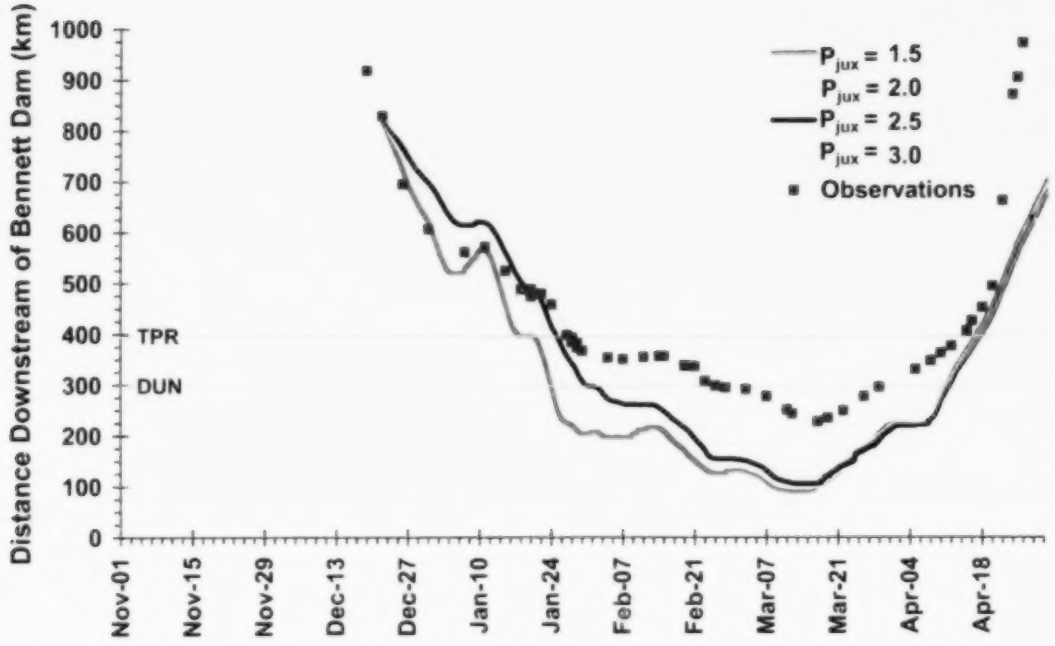

Figure 10 **Peace River ice front profile calibration – 2002/03**

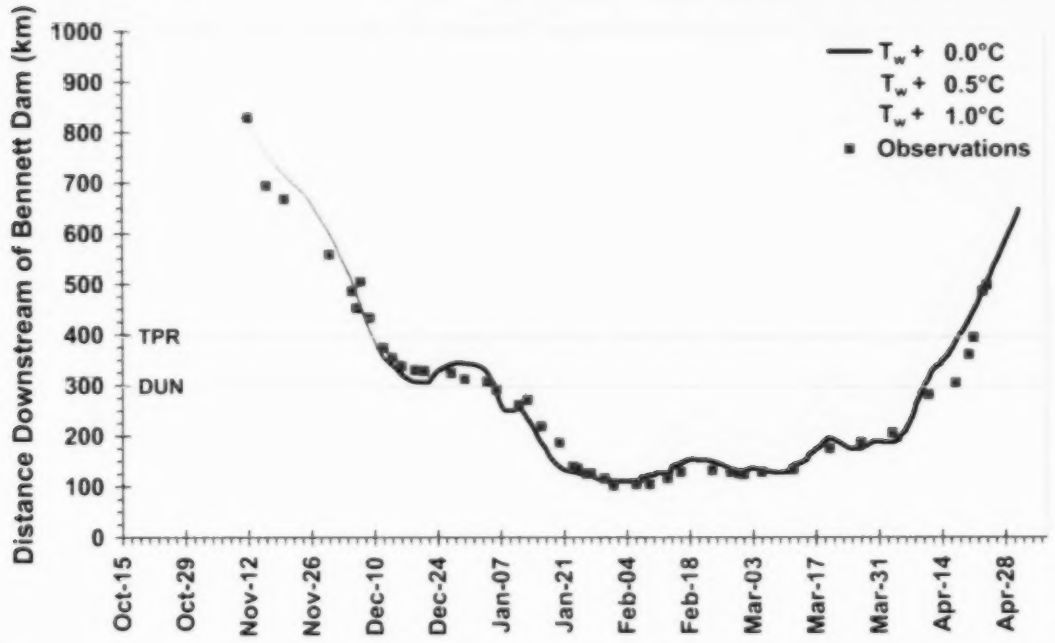

Figure 11 **Effect of reservoir warming on the simulated ice front profile using 1995/96 ice season data**

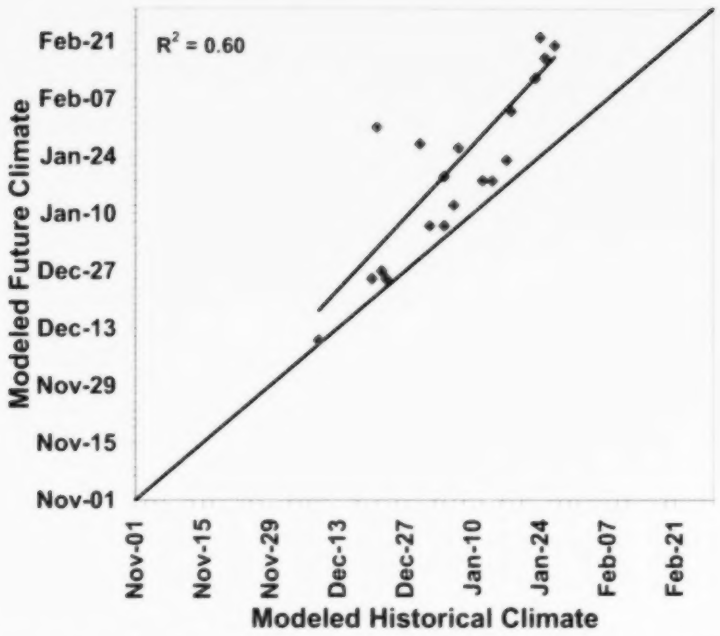

Figure 12 **Modeled historical versus future climate change date of freezeup at the town of Peace River, Alberta**

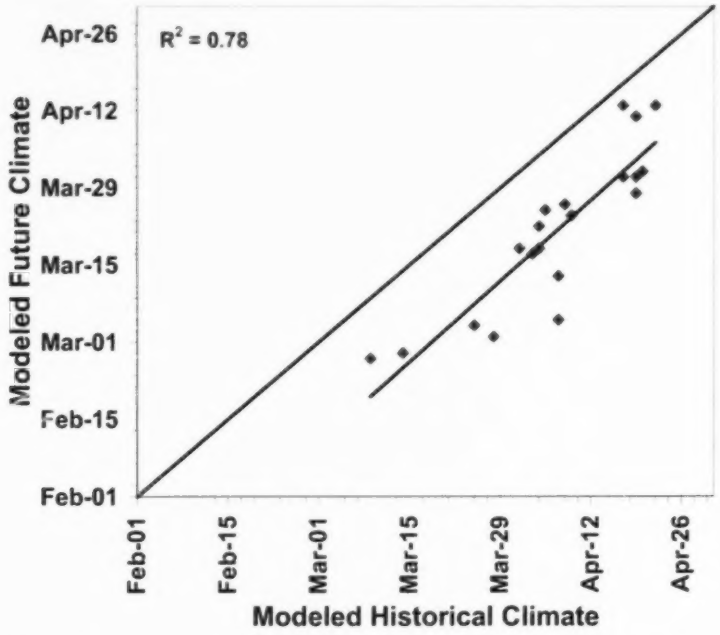

Figure 13 **Modeled historical versus future climate change date of breakup at the town of Peace River, Alberta**

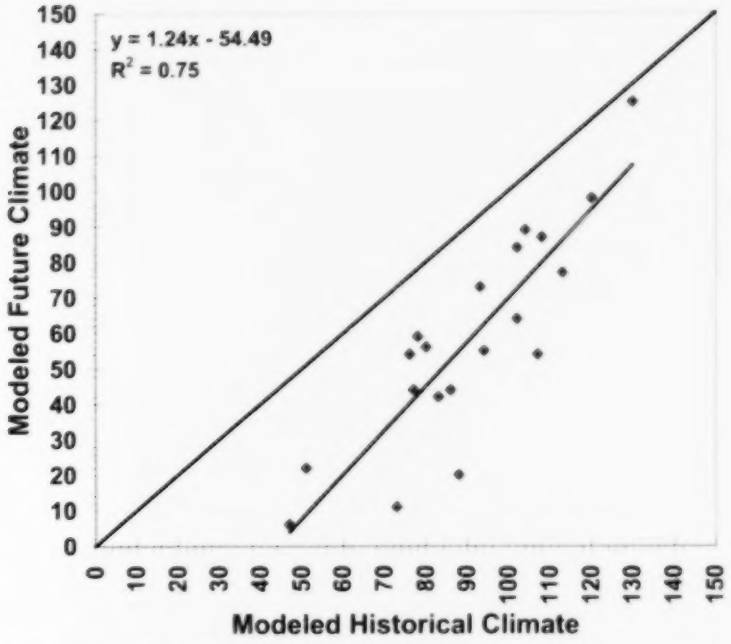

Figure 14 **Modeled historical versus future climate change duration of ice cover (in days) at the town of Peace River, Alberta**

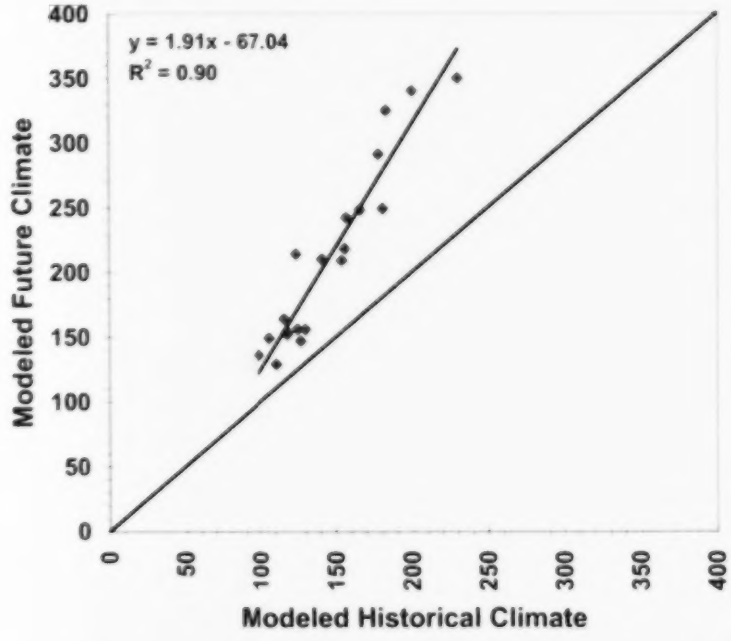

Figure 15 **Modeled historical versus future climate change minimum ice front distance (in kilometres) from the Bennett Dam in British Columbia**

6.0 CONCLUSIONS AND RECOMMENDATIONS

The purpose of this investigation was to apply the *River1D* thermal ice process model to the Peace River and to assess the potential impacts of climate change on its thermal ice regime. The *River1D* hydrodynamic model of the Peace River was based on approximate channel geometry developed and verified in earlier investigations. The model domain extended from the WSC gauge at Hudson Hope (5 km downstream of the Peace Canyon Dam), to Fort Vermilion, where bridging typically occurs at freeze-up.

The primary data for calibration of the thermal ice model was obtained through Alberta Environment. This consisted of detailed input data describing air temperature as well as inflow discharge and water temperature. Validation data used primarily consisted of observed ice front profiles for the most recent 20 years of record, 1984/85 through 2003/04. More detailed validation data were also available for the last two winters, including water temperature at the WSC gauges at Alces and the town of Peace River as well as approximate measurements of some of the ice parameters.

In general, it was found that the *River1D* thermal ice process model produced reasonable predictions of ice cover progression for the validation period, when taking into account the limited input data available (particularly the limited available data describing the inflow water temperature boundary condition). However, because the model was capable of modeling thermal ice processes only, it could not precisely capture ice cover progression in years where dynamic processes, (e.g. ice cover consolidation events) significantly influenced the progression of the ice front. Nevertheless, the model's capability is considered quite adequate for the purposes of this preliminary study.

To explore the potential impacts of climate change on the Peace River ice regime, the validated model was then applied for the same period, using the air temperature changes indicated for Fort St. John, the town of Peace River, and High Level under the A2 climate change projection for the year 2050, generated by the CGCM2 model. An important consideration affecting the interpretation of these results is that increased air temperatures would also potentially have an impact on the upstream boundary water temperature condition (i.e. by increasing the reservoir water temperatures) and would likely delay the time of first ice formation at the downstream boundary (i.e. the bridging date). Both these effects would tend to delay the progression of the ice cover and possibly lead to earlier thermal melt. Thus, in this context, the results indicated here are likely conservative in that they may underestimate the degree of this particular climate change scenario's potential impact on the Peace River ice regime.

Results of this preliminary climate change impact assessment suggest that there is a significant potential for a reduced ice covered season under the climate change scenario investigated. In terms of the delay in the date of freezeup at the town of Peace River, an average of 16 days was indicated and for breakup, the average date was 17 days earlier. These results amount to a 33-day reduction in duration of ice cover at the town of Peace River. In addition, the simulated maximum ice cover extent was an average of 66 kilometres shorter after climate change, compared to the historical simulation results.

Given the limited input and validation data, the fact that the model only considers thermal ice processes at this time, the lack of consideration of the effects of climate change on reservoir outflow temperatures and ice cover initiation date, and uncertainties associated with the meteorological climate change analysis itself (as well as its applicability for this particular period of record), these quantitative averages cannot be considered firm predictions. However, their magnitudes do definitely suggest that there will be a measurable, and possibly even significant, impact attributable to climate change on the future ice regime of the Peace River. Therefore, it is important now to start developing adaptive strategies as well as improved models and data archives, in order to gain a more reliable quantitative assessment of these impacts.

In terms of the latter two issues, the following recommendations are suggested:

- the *River1D* model should be extended to include dynamic ice effects, thus improving its ability to quantitatively assess Peace River ice conditions;
- the current intensive ice monitoring program on the Peace River should be continued as long as possible, and at the very least for a total of 5 years, to ensure adequate calibration data can be obtained;
- additional water temperature data sites along the river would provide extremely useful calibration and validation data;
- the inflow water temperatures (i.e. reservoir outflow temperatures) should continue to be monitored even after the intensive ice monitoring program is discontinued;
- reservoir models should be developed to assess the potential impacts of climate change on reservoir outflow water temperatures on the Peace River;
- although no deterministic model for bridging presently exists, one is necessary to fully assess the potential impacts of climate change on the winter regime of the Peace River, as delayed bridging under future climate conditions would be expected to have a significant impact on the progression of the ice front; and
- since there is a considerable amount of uncertainty in the socio-economic predictions used to develop the future climate scenario applied, additional scenarios (such as the less-severe B2 scenario) should be investigated to establish a range of possible climate change effects.

7.0 LITERATURE CITED

Andres, D.D. (1993) "Effects of Climate Change on the Freezeup Regime of the Peace River: Phase I Ice Production Algorithm Development and Calibration", Report No. SWE 93/01, Environmental Research & Engineering Department, Alberta Research Council, Edmonton, Alberta, 52 pp.

Blackburn, J. and Hicks, F. (2002) "Combined Flood Routing and Flood Level Forecasting", Canadian Journal of Civil Engineering, 29(1): 64-75.

Chemical Rubber Company (CRC) (2004) "CRC Handbook of Chemistry and Physics, 84th Edition", Online resource, http://www.library.ualberta.ca/databases/databaseinfo/index.cfm?ID=3193.

Hicks, F.E. and Steffler, P.M. (1990) "Finite Element Modeling of Open Channel Flow" Water Resources Engineering Report No. 90-6, Department of Civil Engineering, University of Alberta, Edmonton, Alberta, 383 pp.

Hicks, F.E. and Steffler, P.M., (1992) "A Characteristic-Dissipative-Galerkin Scheme for Open Channel Flow", ASCE Journal of Hydraulic Eng., 118(2): 337-352.

Hicks, F.E. and McKay, K. (1995) "Peace/Slave River Flow Modeling" Water Resources Engineering Report No. 95-H3 (Northern River Basins Study Project 1154-D1), Department of Civil Engineering, University of Alberta, Edmonton, Alberta, 175 pp.

Hicks, F.E. (1996) "Hydraulic Flood Routing with Minimal Channel Data: Peace River, Canada", Canadian Journal of Civil Engineering, 23(2): 524-535.

Kellerhals, R., Neill, C.R., and Bray, D.I. (1972) "Hydraulic and Geomorphic Characteristics of Rivers in Alberta", River Engineering and Surface Hydrology Report 72-1, Alberta Research Council, Edmonton, Alberta.

Shen, H.T., Wang, S., and Lal, A.M.W. (1995) "Numerical Simulation of River Ice Processes", Journal Cold Regions Eng., Vol. 9, No. 3, 107-118.

Wasantha Lal, A.M., and Shen, H.T. (1989) "A Mathematical Model for River Ice Processes (RICE)", Report No. 89-4, Department of Civil and Environmental Engineering, Clarkson University, Potsdam, New York, 164 pp.

APPENDIX A

Simulated Historical Ice Front Profiles (1984/85 through 2003/04)

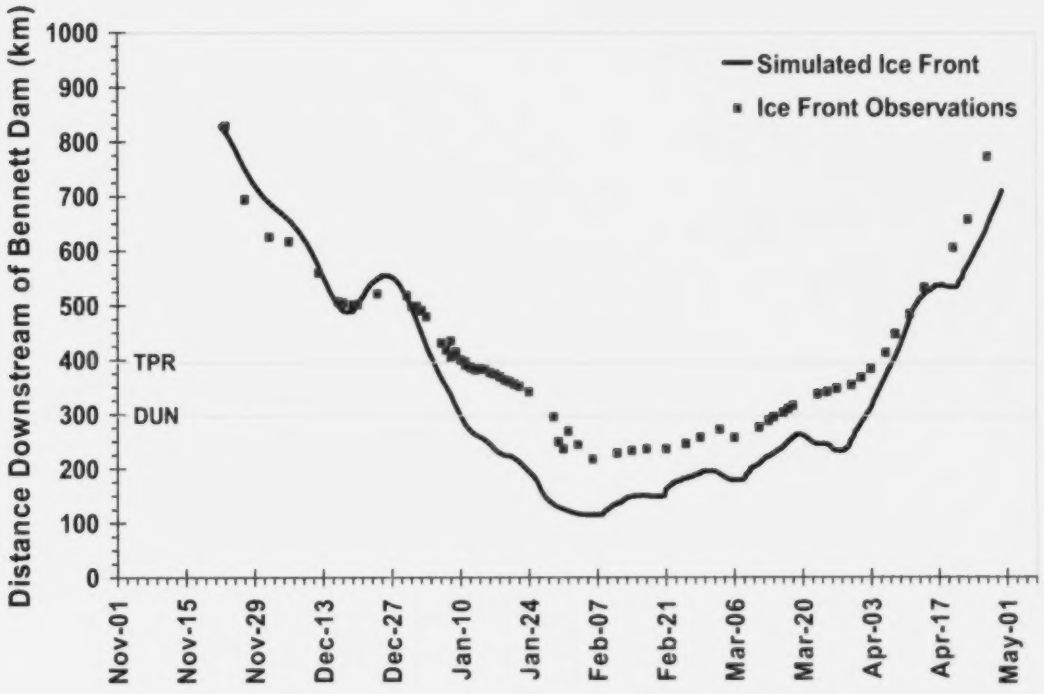

Figure A-1 Modeled and observed ice front profile – 2003/04

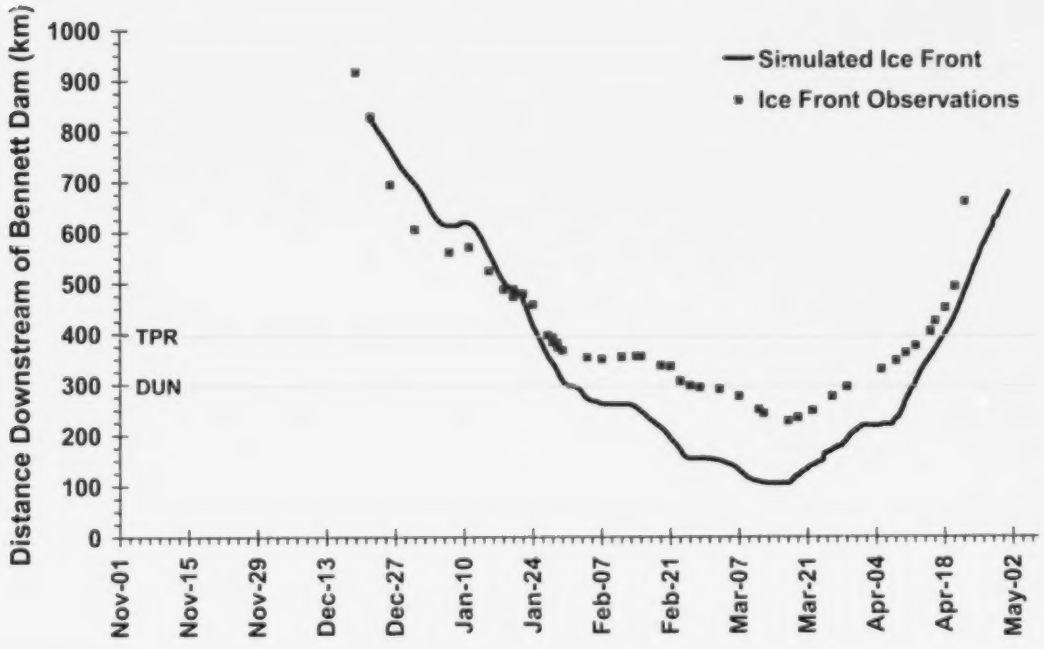

Figure A-2 Modeled and observed ice front profile – 2002/03

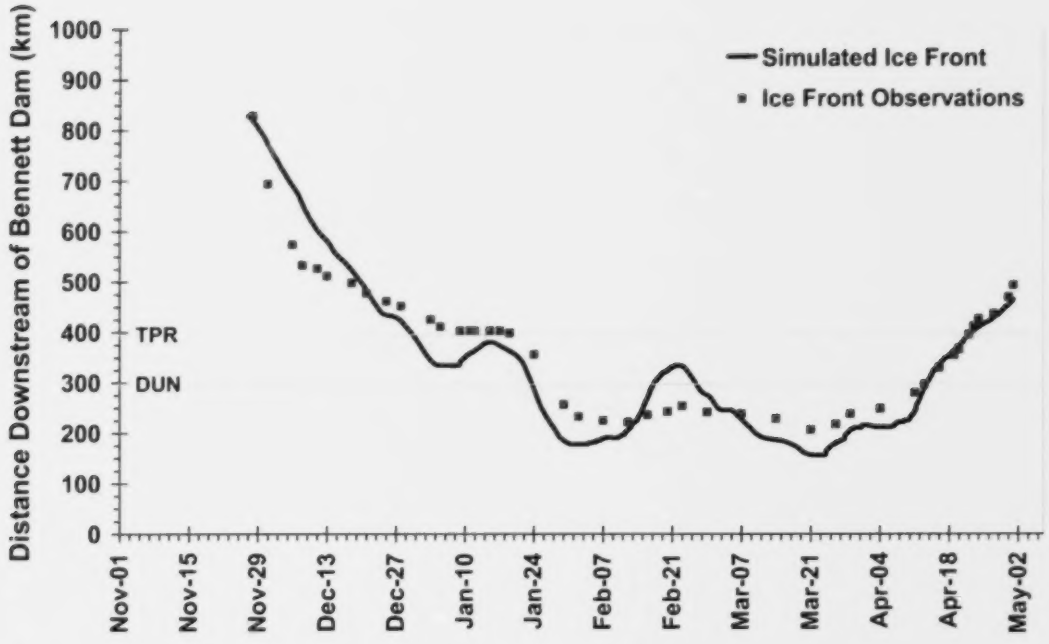

Figure A-3 Modeled and observed ice front profile – 2001/02

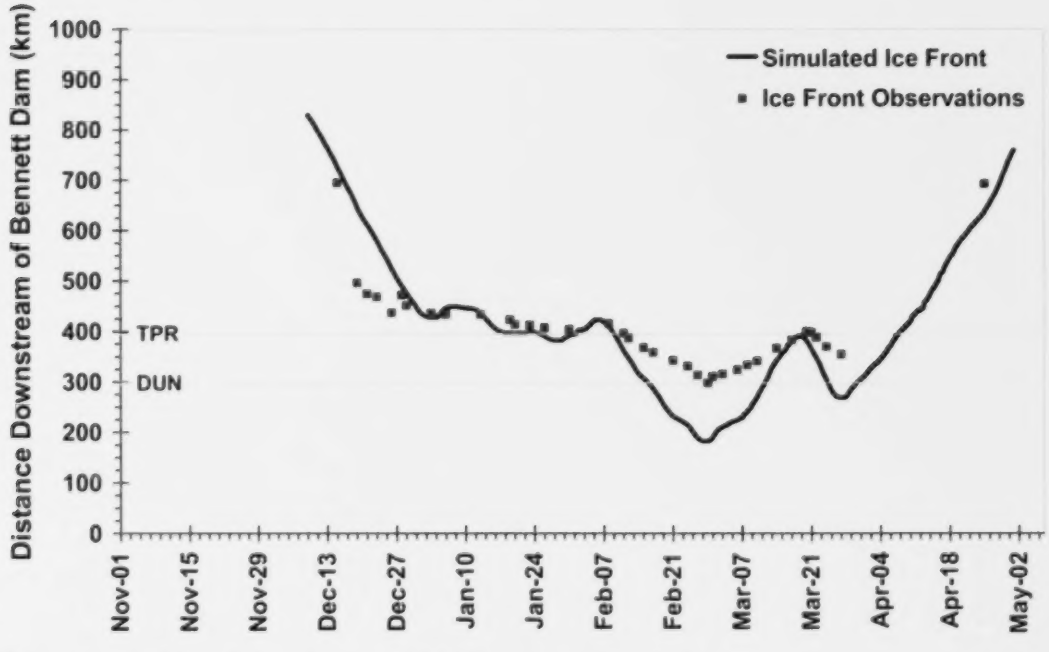

Figure A-4 Modeled and observed ice front profile – 2000/01

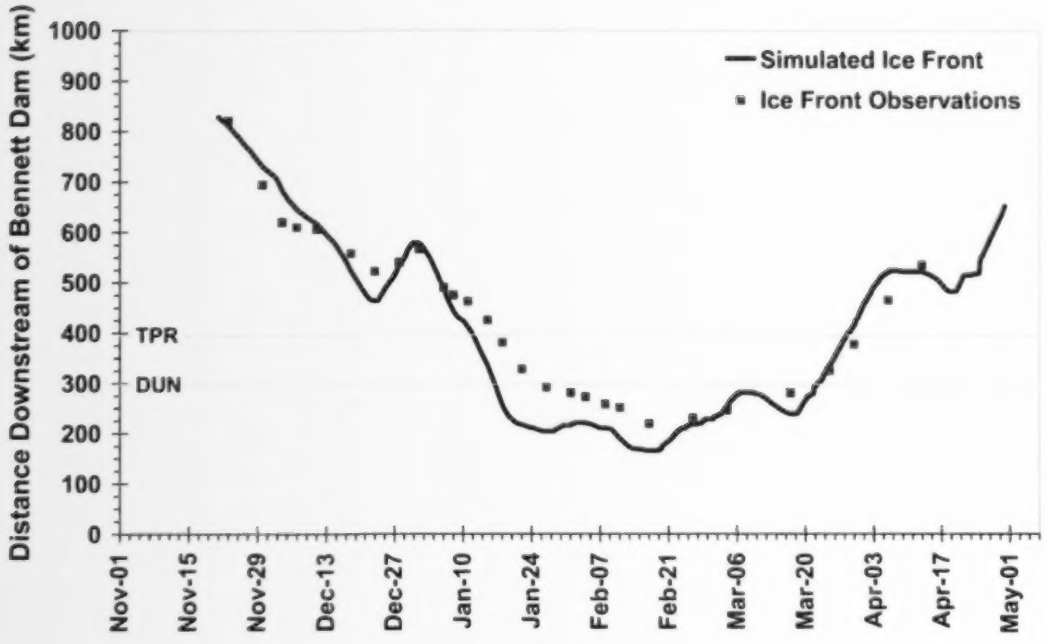

Figure A-5 Modeled and observed ice front profile – 1999/00

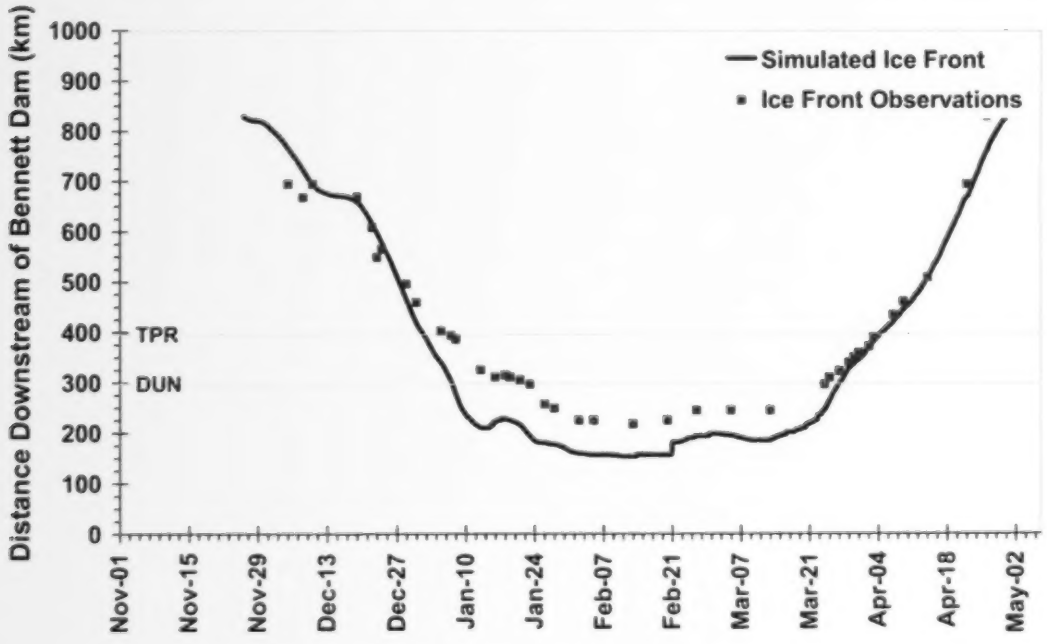

Figure A-6 Modeled and observed ice front profile – 1998/99

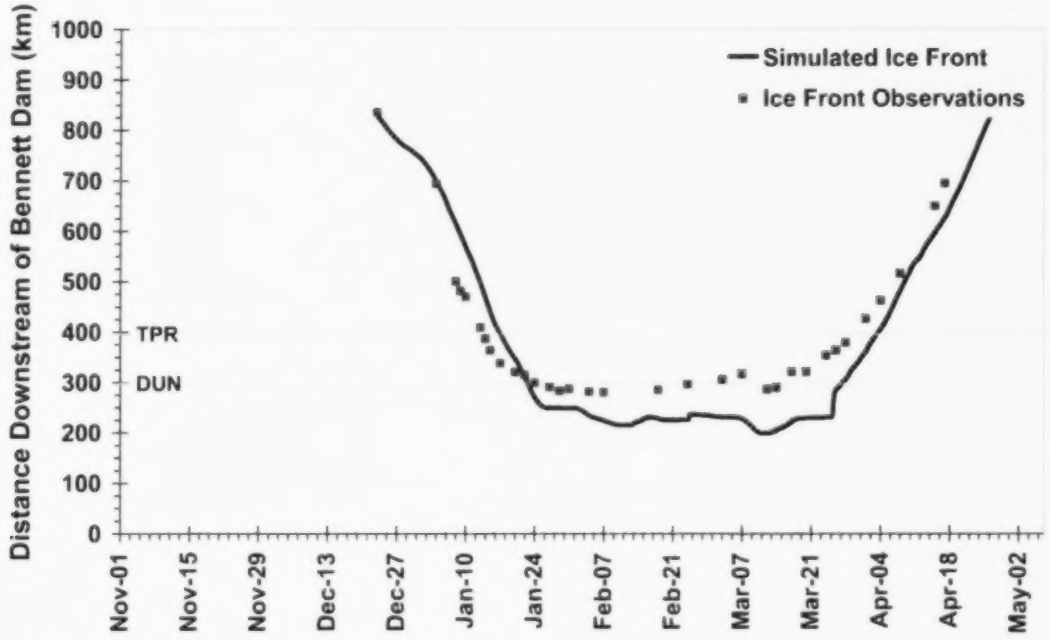

Figure A-7 Modeled and observed ice front profile – 1997/98

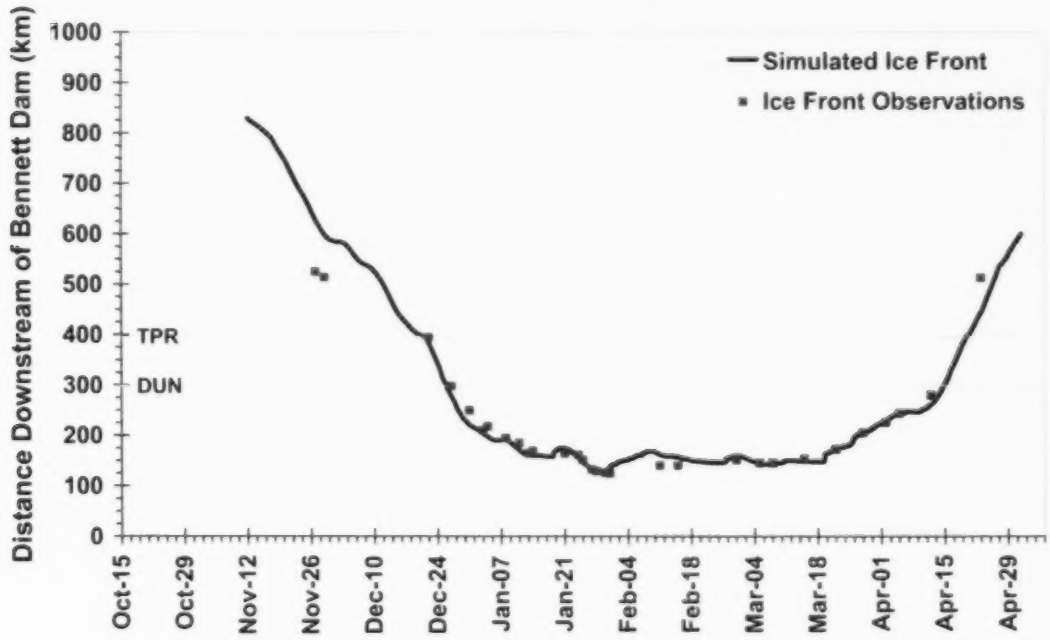

Figure A-8 Modeled and observed ice front profile – 1996/97

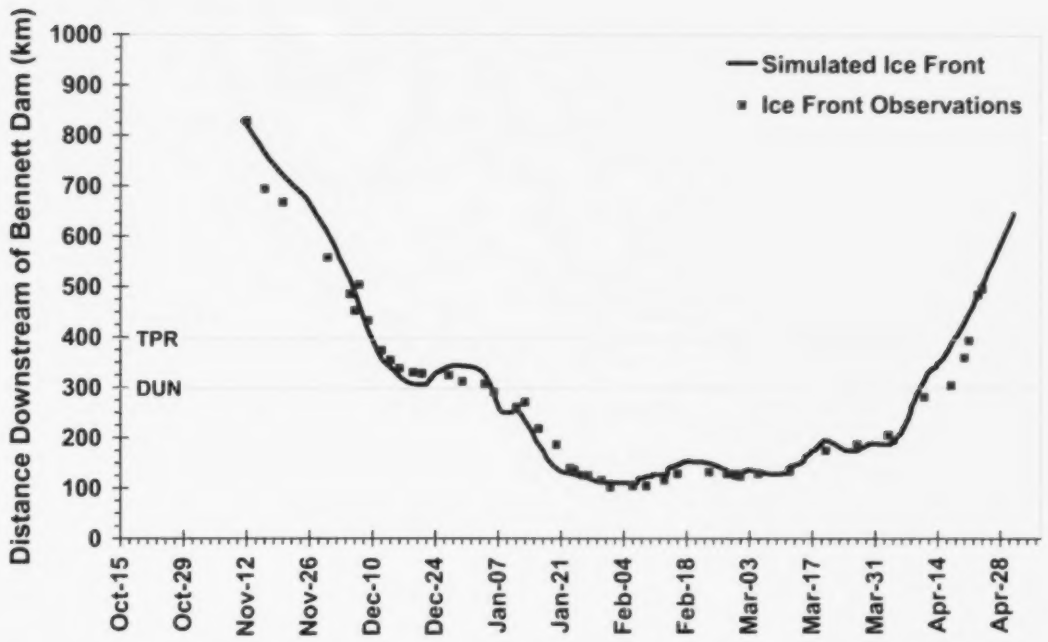

Figure A-9 Modeled and observed ice front profile – 1995/96

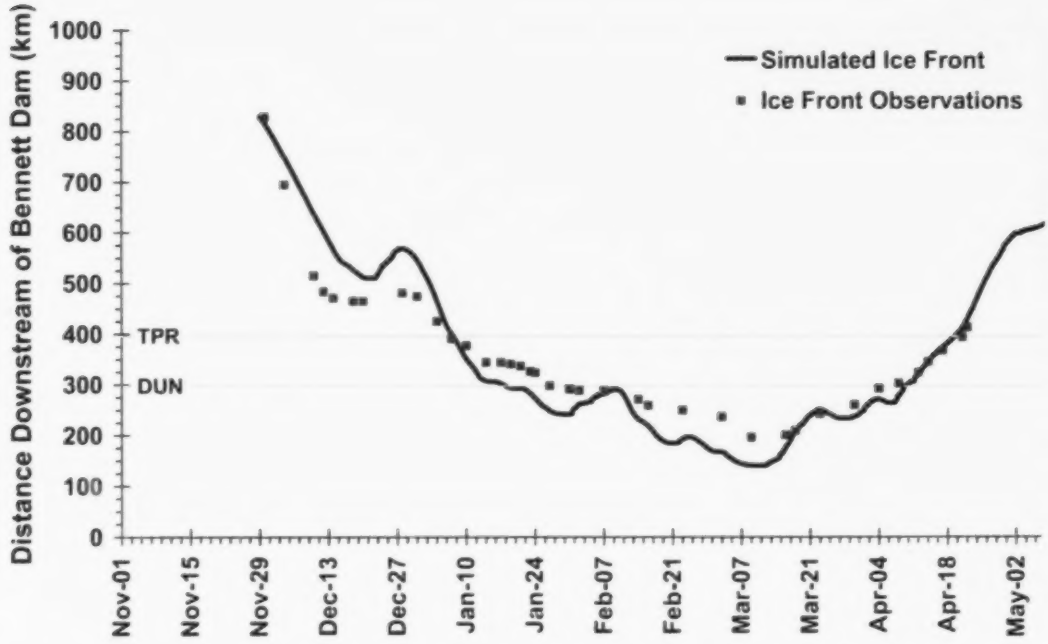

Figure A-10 Modeled and observed ice front profile – 1994/95

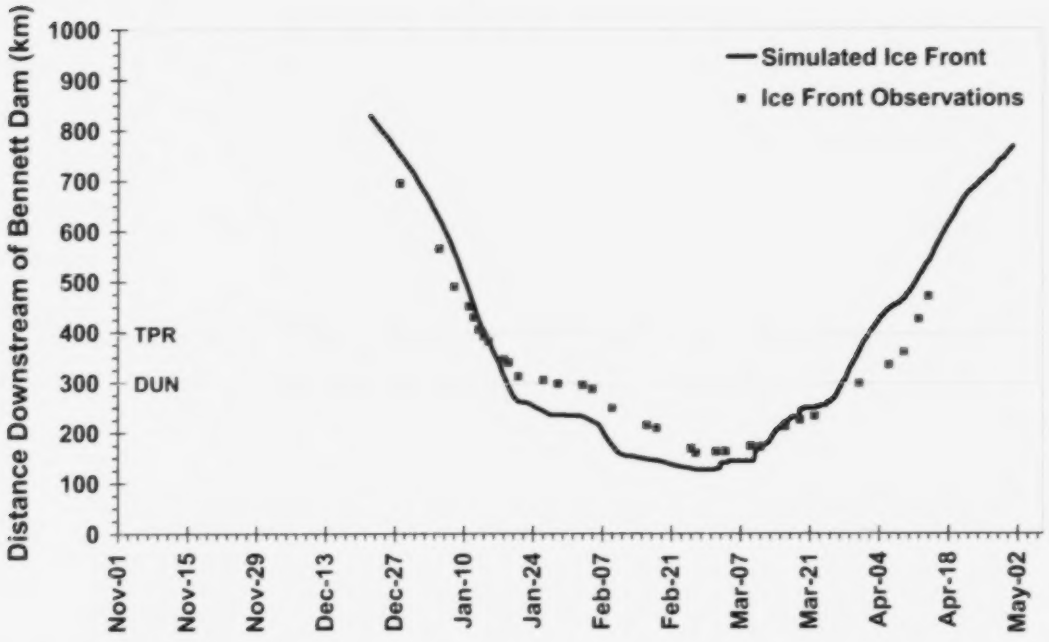

Figure A-11 Modeled and observed ice front profile – 1993/94

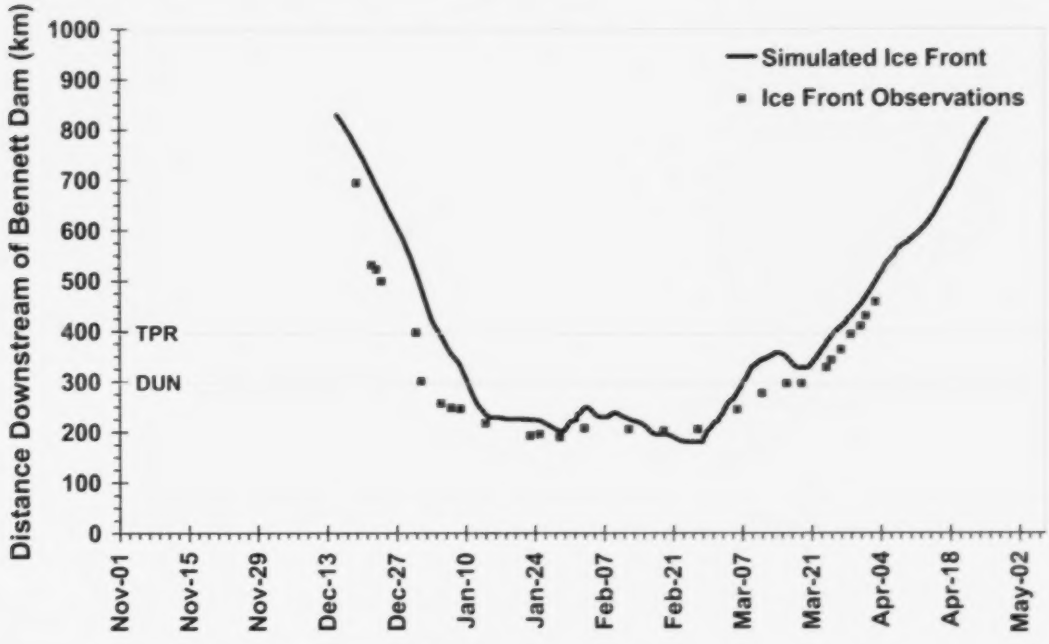

Figure A-12 Modeled and observed ice front profile – 1992/93

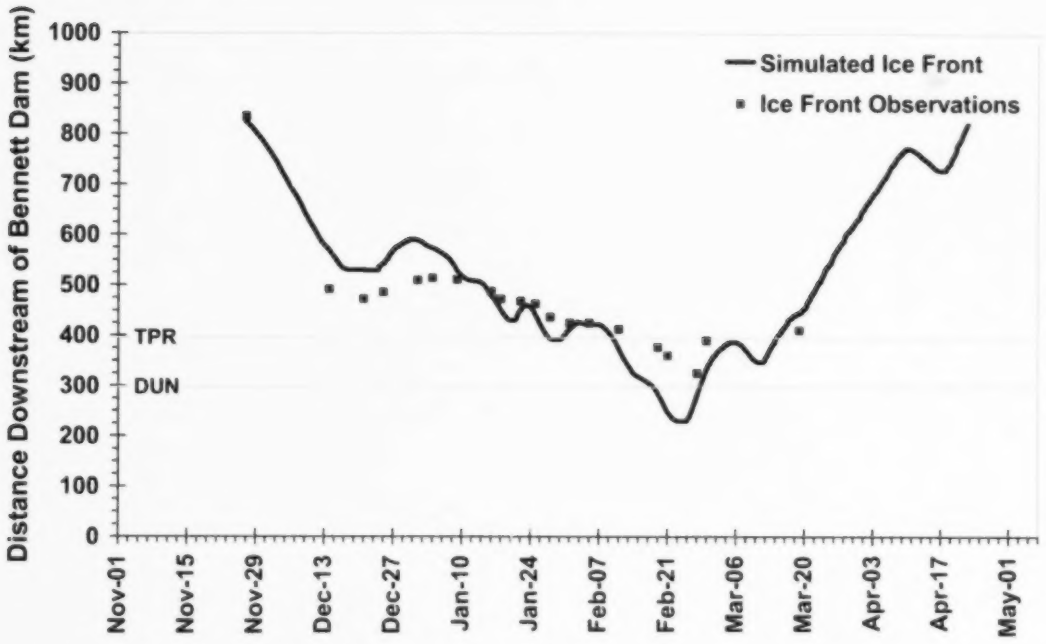

Figure A-13 Modeled and observed ice front profile – 1991/92

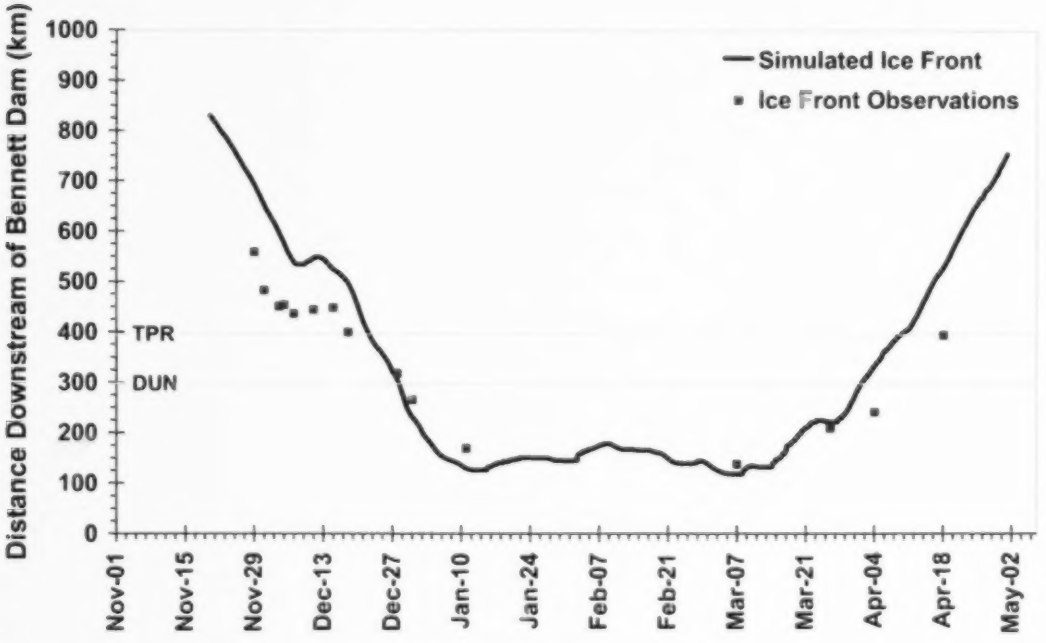

Figure A-14 Modeled and observed ice front profile – 1990/91

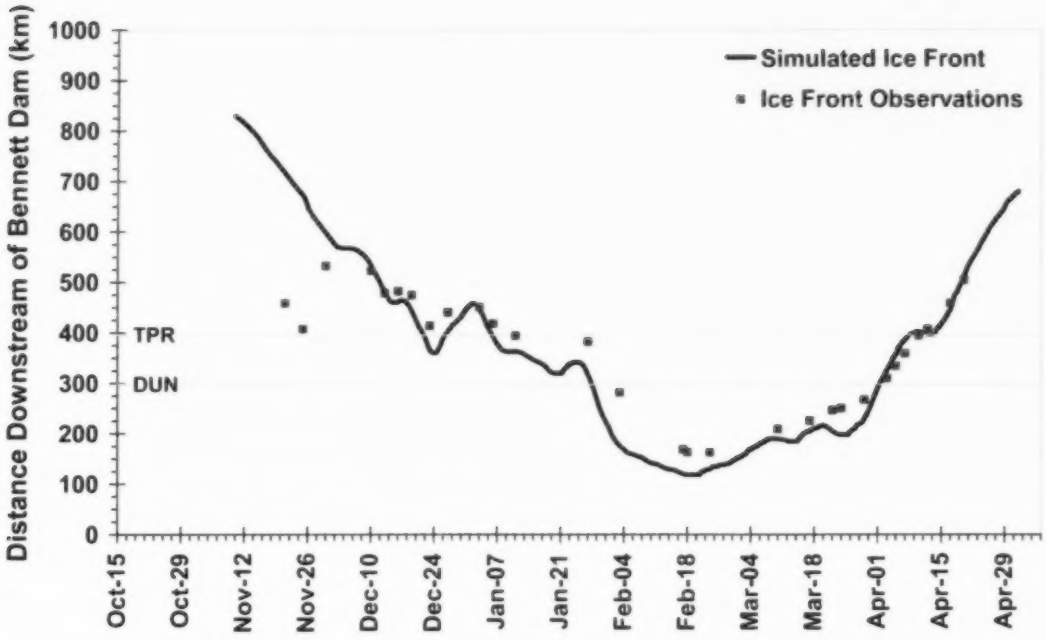

Figure A-15 Modeled and observed ice front profile – 1989/90

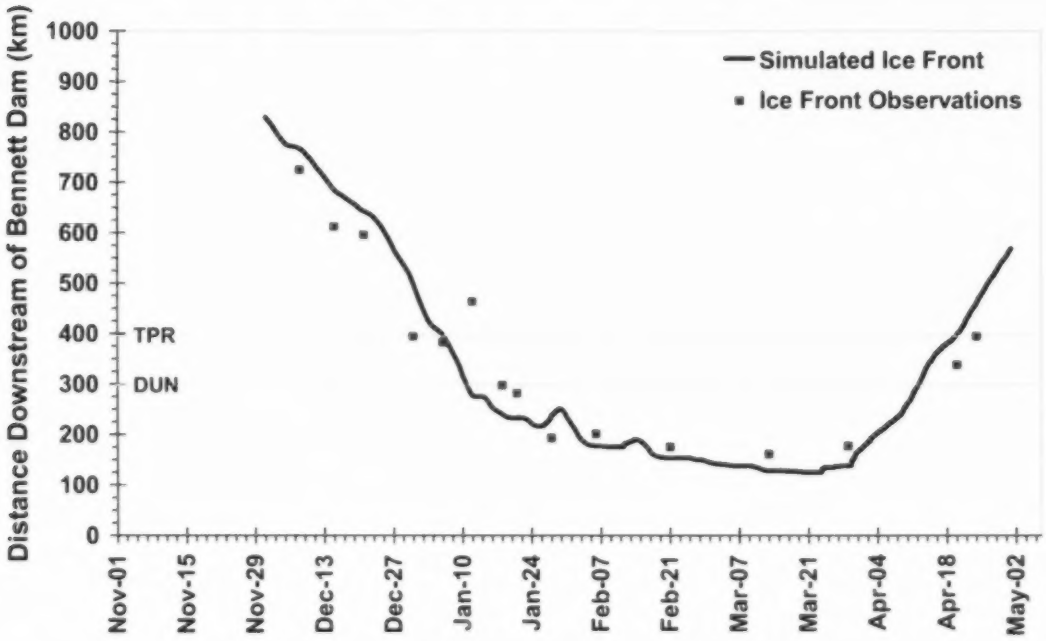

Figure A-16 Modeled and observed ice front profile – 1988/89

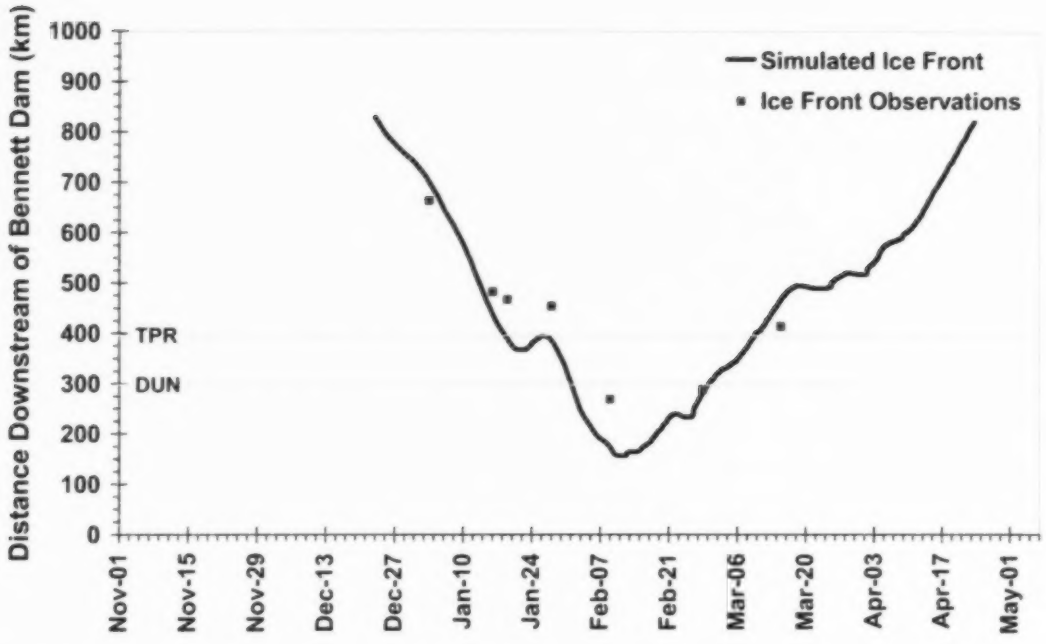

Figure A-17 Modeled and observed ice front profile – 1987/88

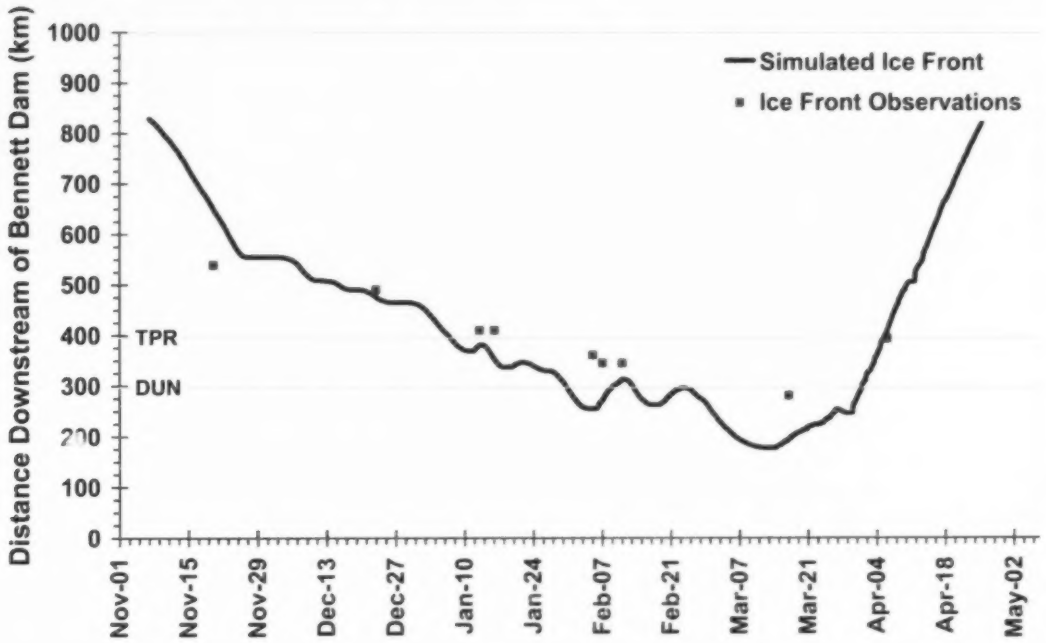

Figure A-18 Modeled and observed ice front profile – 1986/87

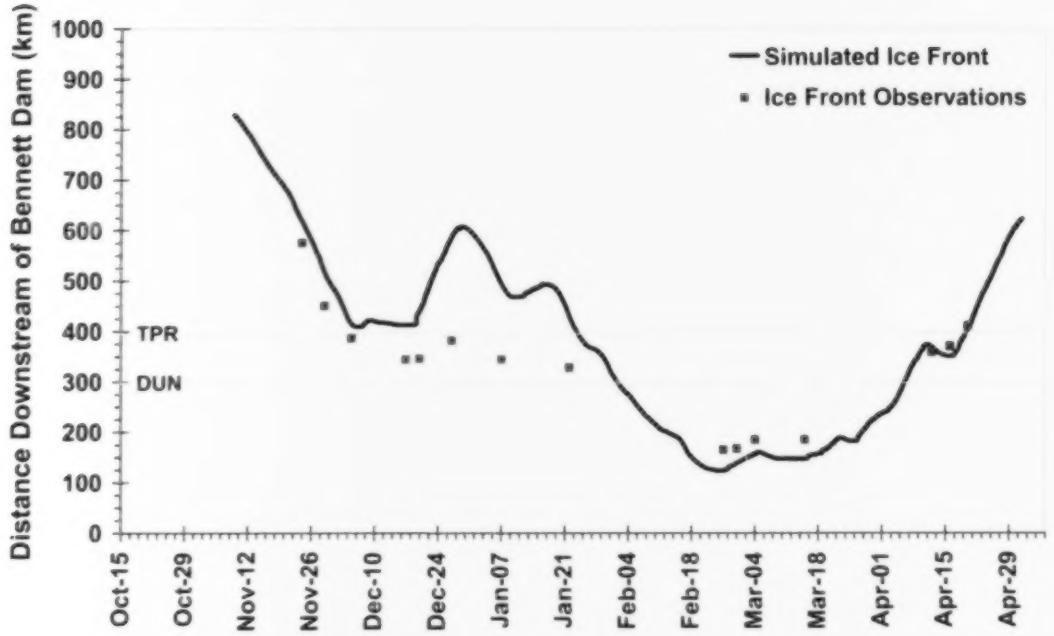

Figure A-19 Modeled and observed ice front profile – 1985/86

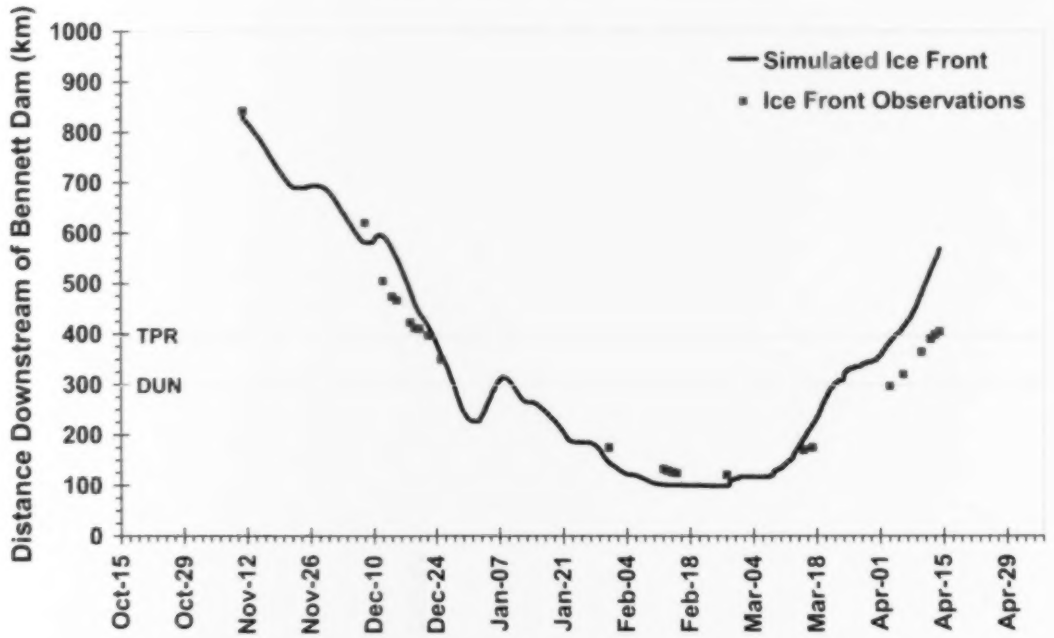

Figure A-20 Modeled and observed ice front profile – 1984/85

APPENDIX B

Simulated Future Climate Ice Front Profiles Compared to Historical (1984/85 through 2003/04)

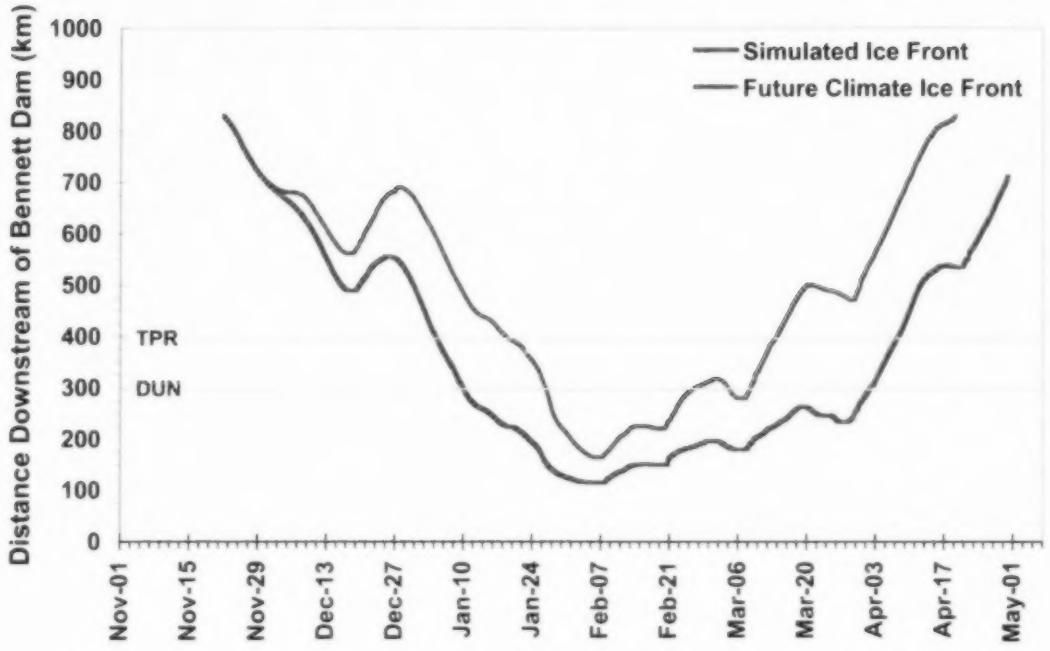

Figure B-1 Historical versus climate change modeled ice front profile – 2003/04

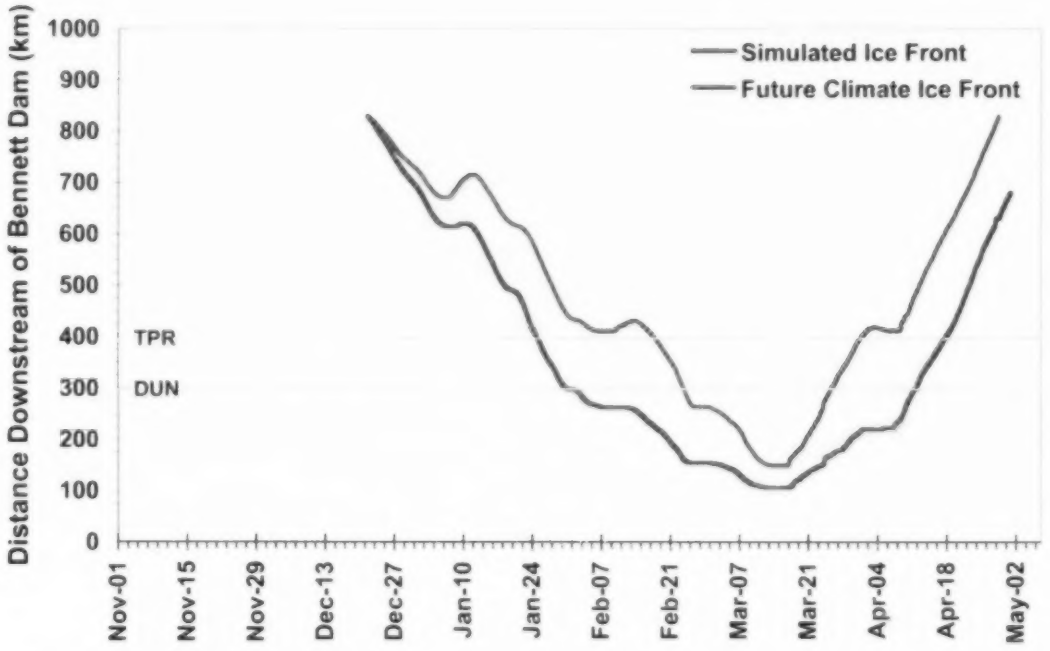

Figure B-2 Historical versus climate change modeled ice front profile – 2002/03

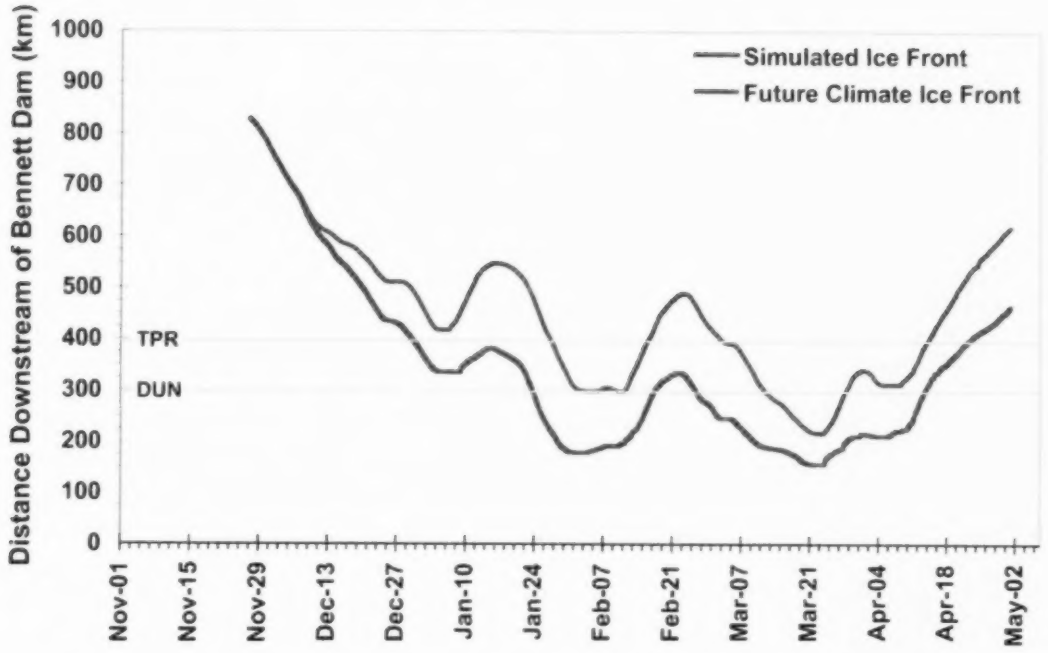

Figure B-3 Historical versus climate change modeled ice front profile – 2001/02

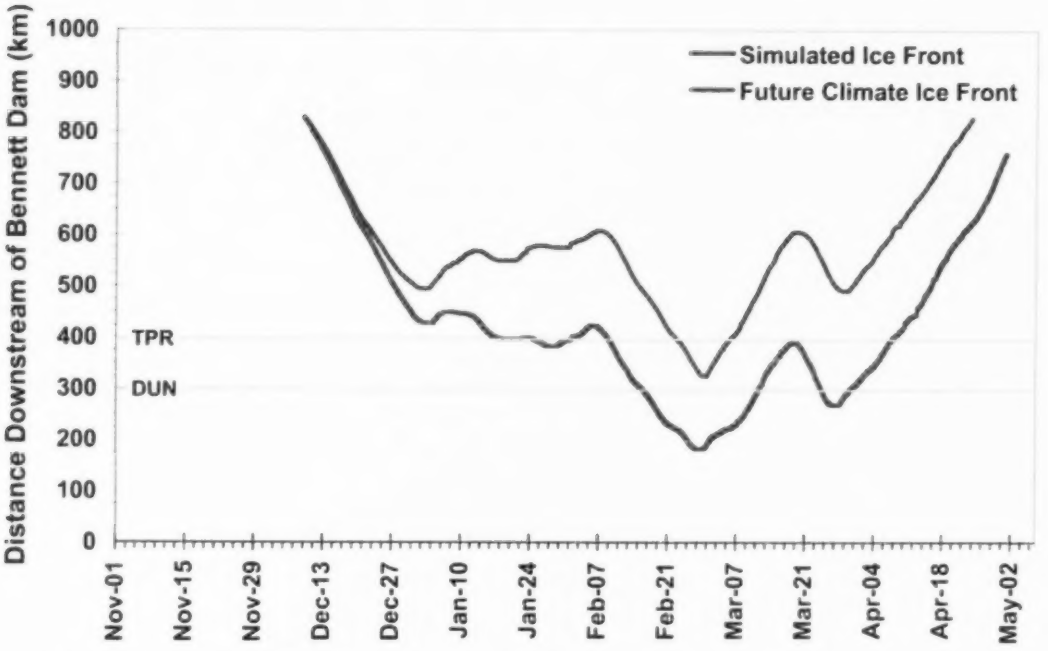

Figure B-4 Historical versus climate change modeled ice front profile – 2000/01

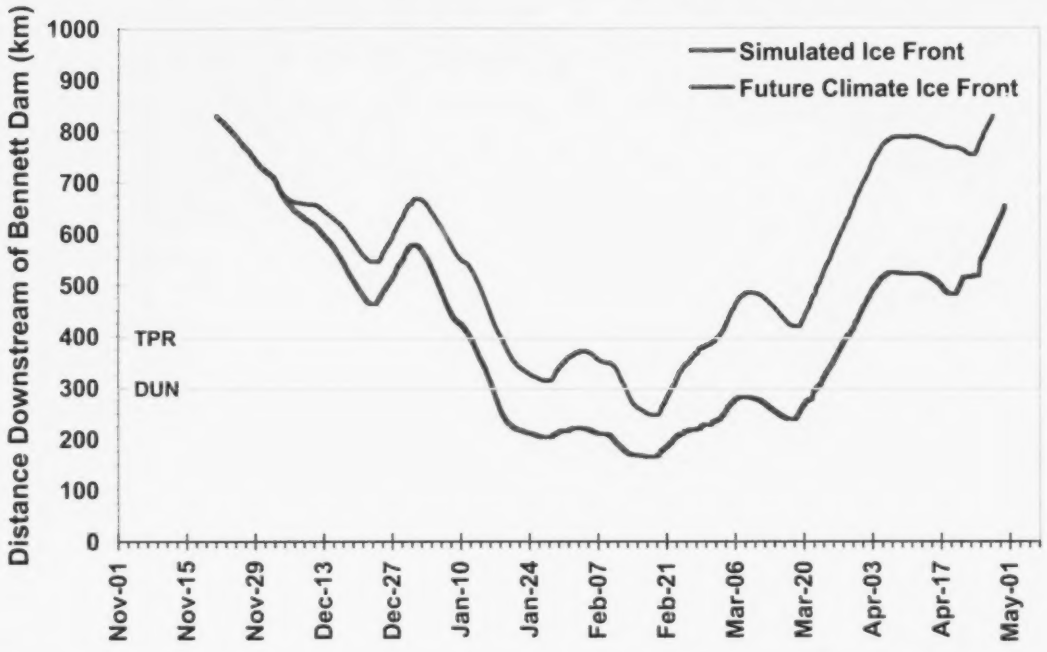

Figure B-5 Historical versus climate change modeled ice front profile – 1999/00

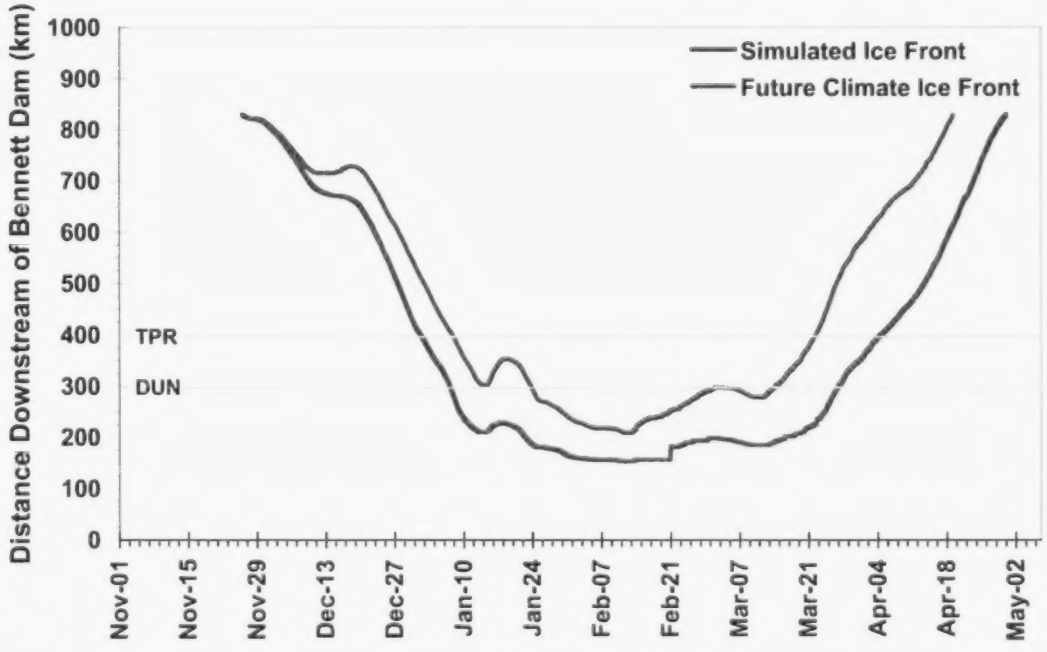

Figure B-6 Historical versus climate change modeled ice front profile – 1998/99

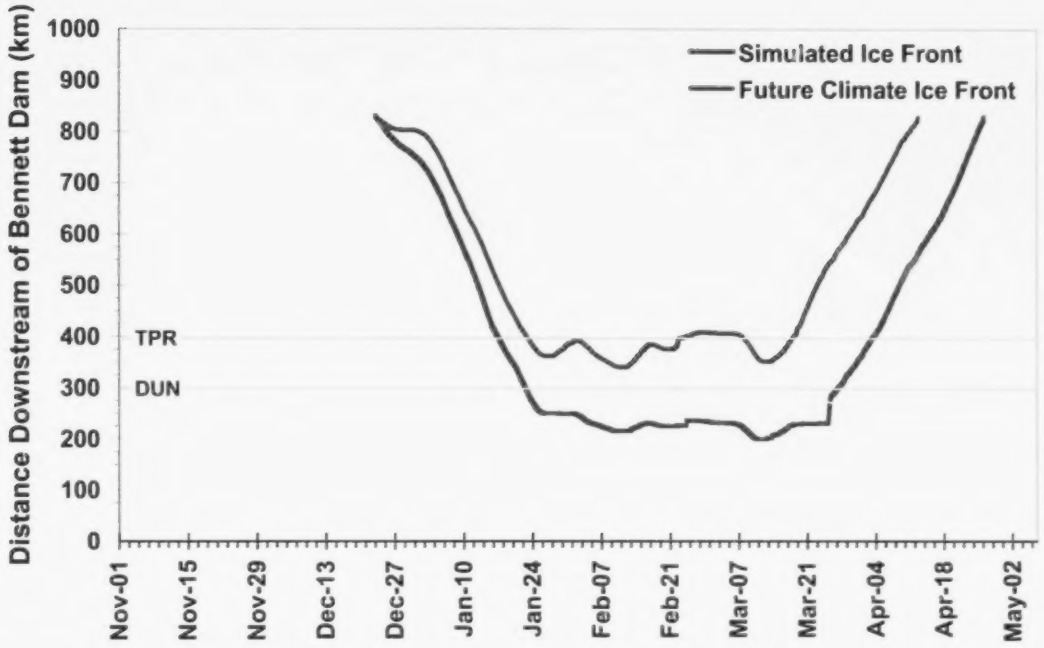

Figure B-7 Historical versus climate change modeled ice front profile – 1997/98

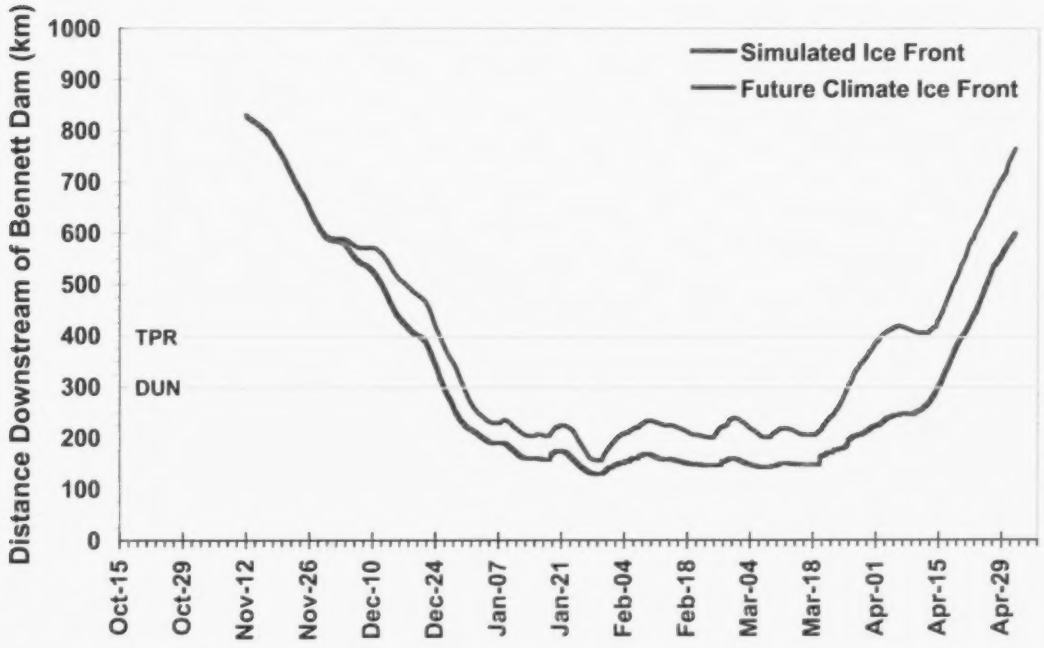

Figure B-8 Historical versus climate change modeled ice front profile – 1996/97

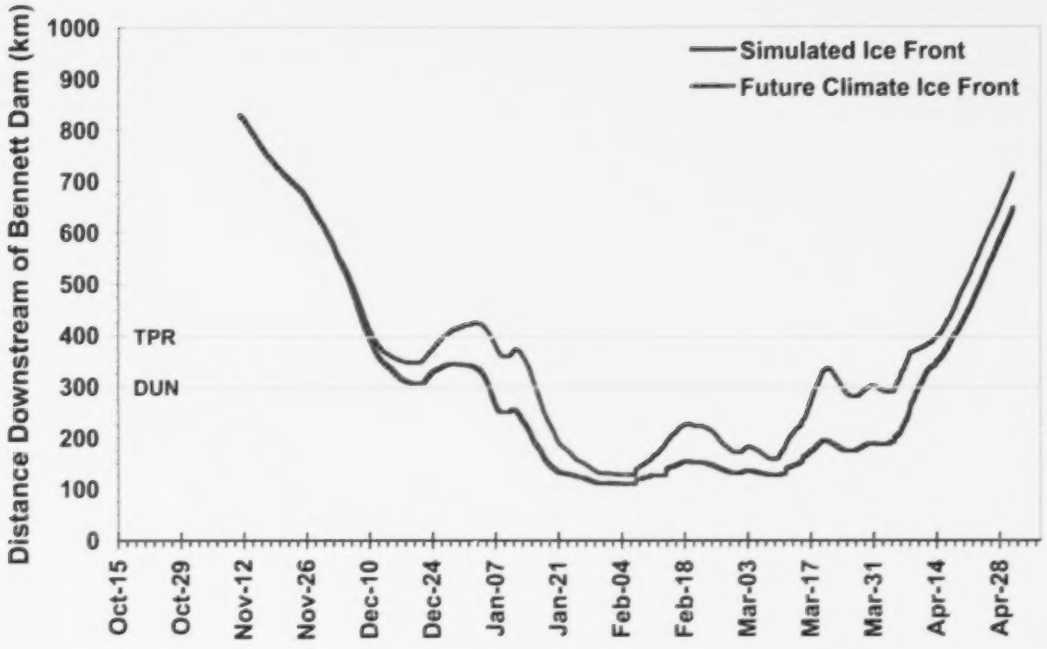

Figure B-9 Historical versus climate change modeled ice front profile – 1995/96

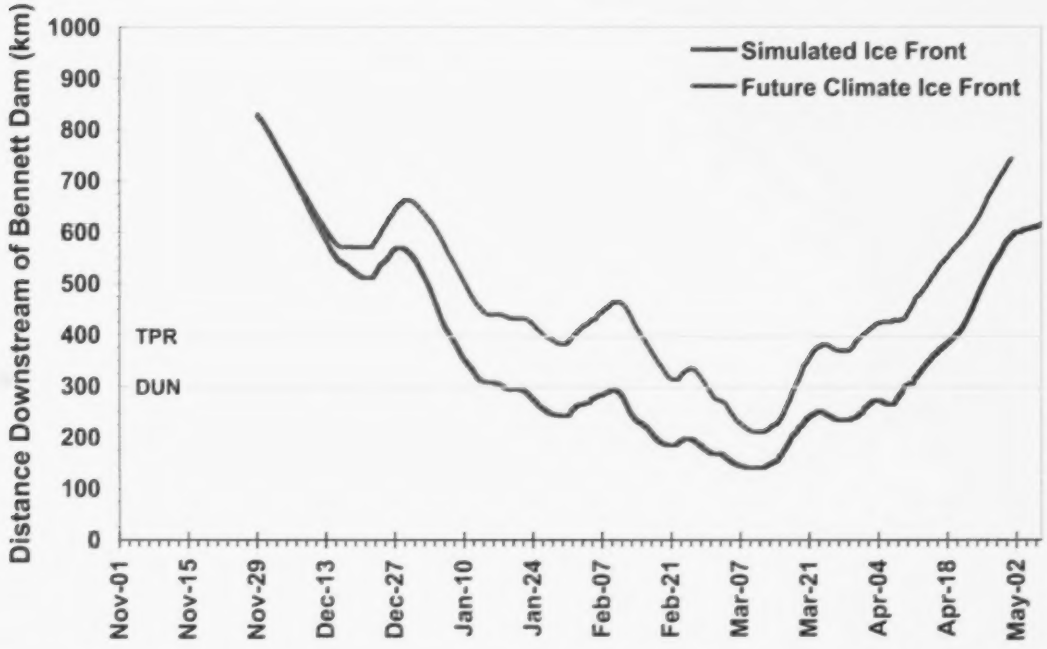

Figure B-10 Historical versus climate change modeled ice front profile – 1994/95

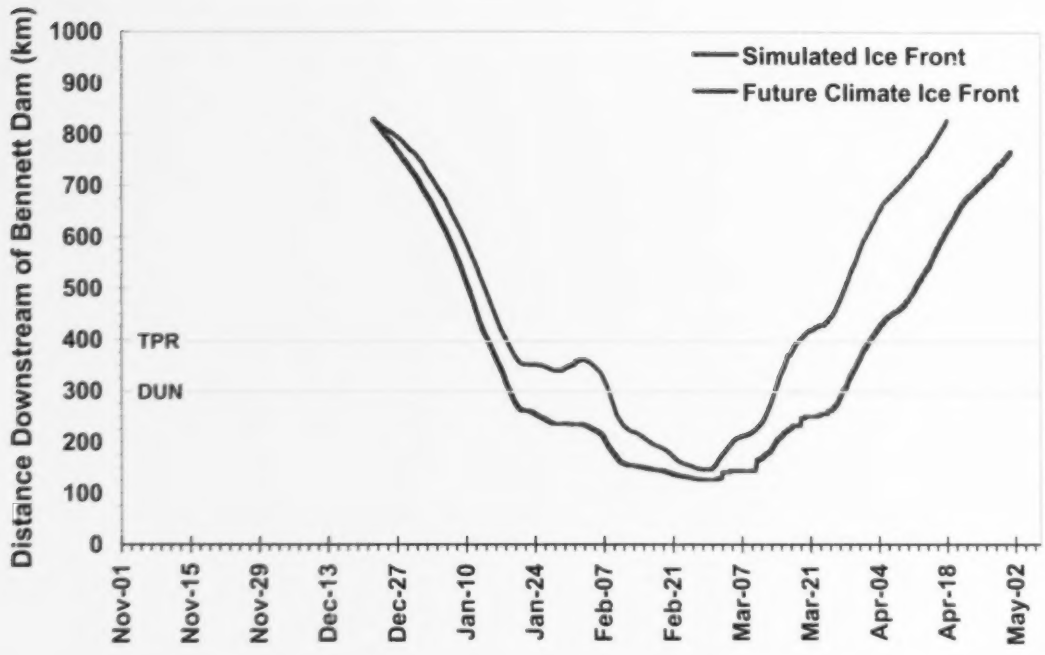

Figure B-11 Historical versus climate change modeled ice front profile – 1993/94

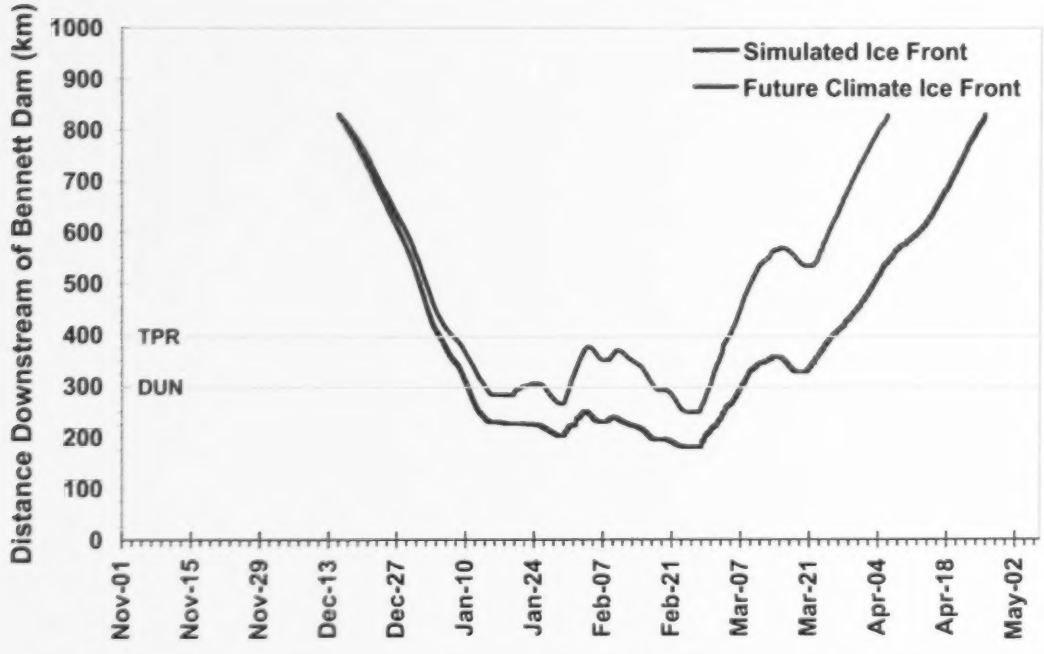

Figure B-12 Historical versus climate change modeled ice front profile – 1992/93

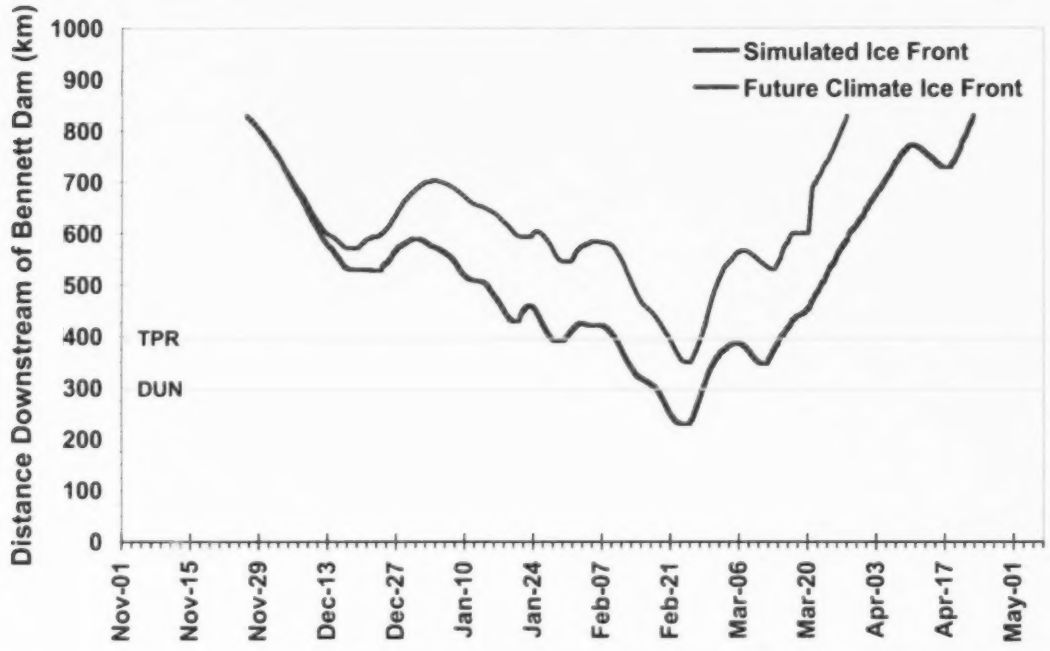

Figure B-13 Historical versus climate change modeled ice front profile – 1991/92

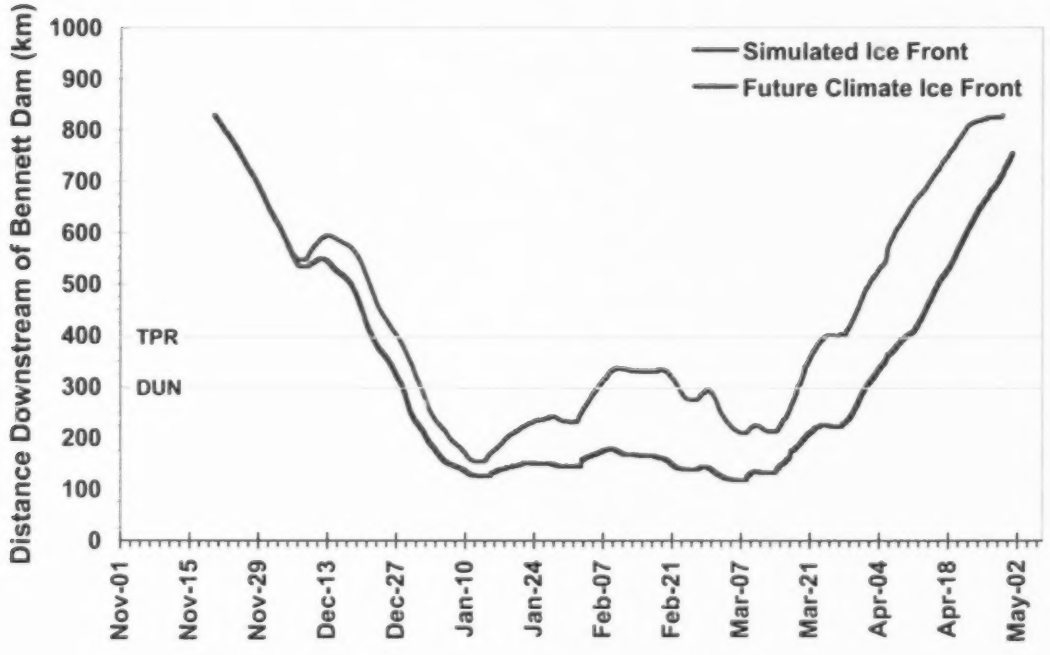

Figure B-14 Historical versus climate change modeled ice front profile – 1990/91

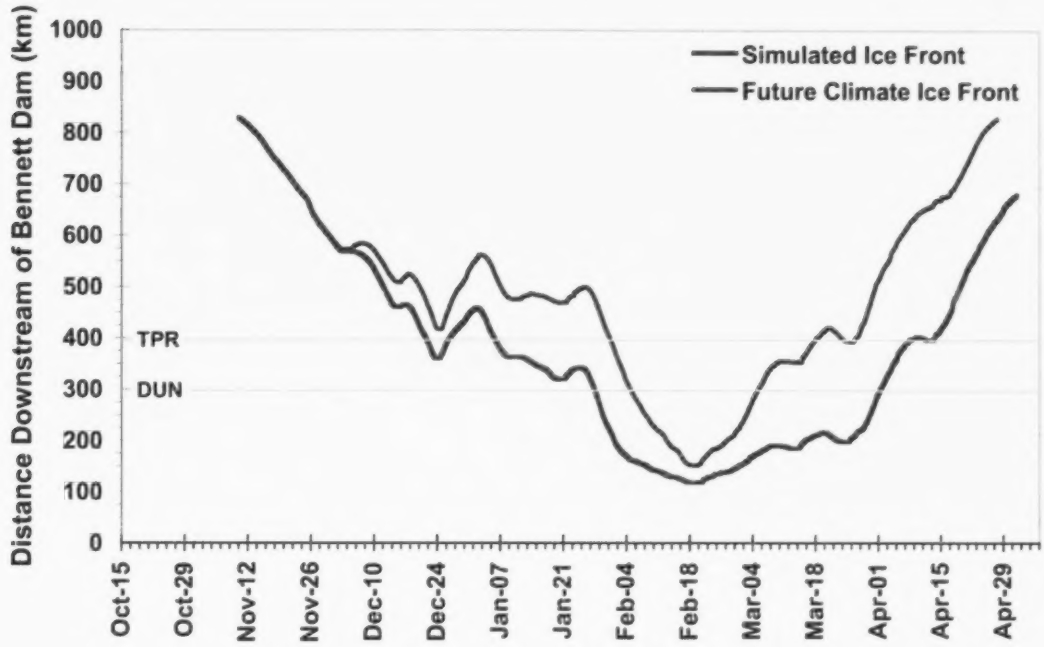

Figure B-15 Historical versus climate change modeled ice front profile – 1989/90

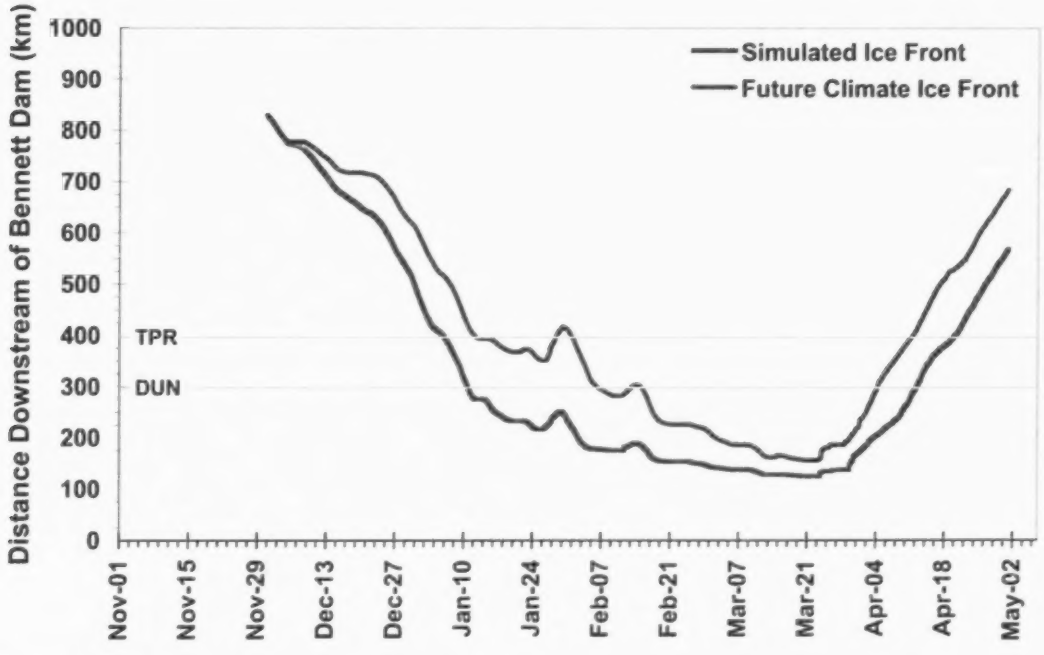

Figure B-16 Historical versus climate change modeled ice front profile – 1988/89

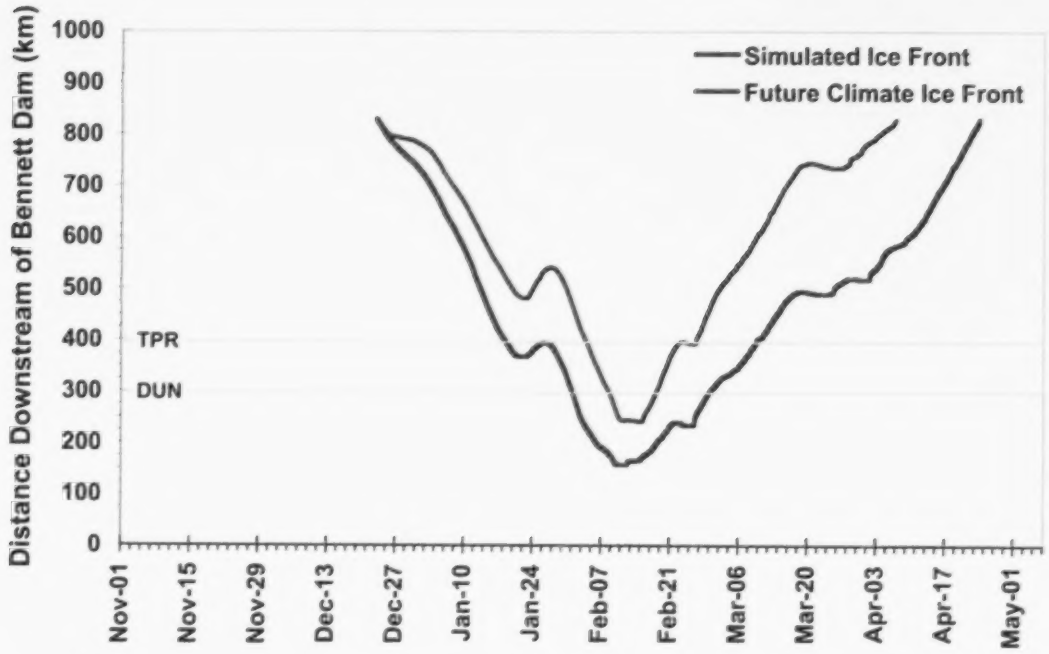

Figure B-17 Historical versus climate change modeled ice front profile – 1987/88

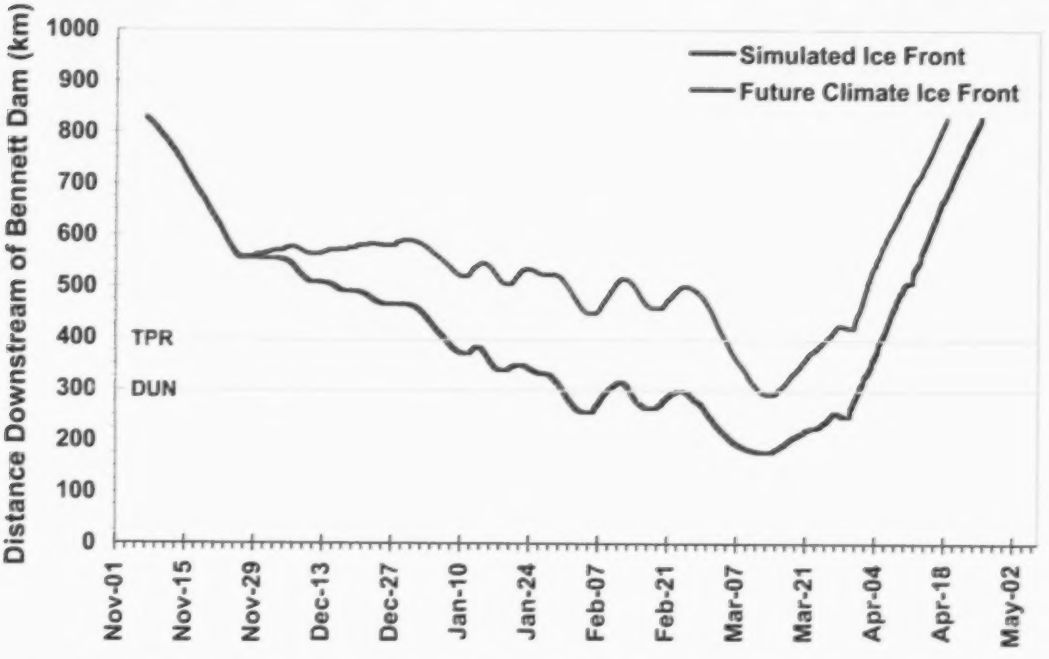

Figure B-18 Historical versus climate change modeled ice front profile – 1986/87

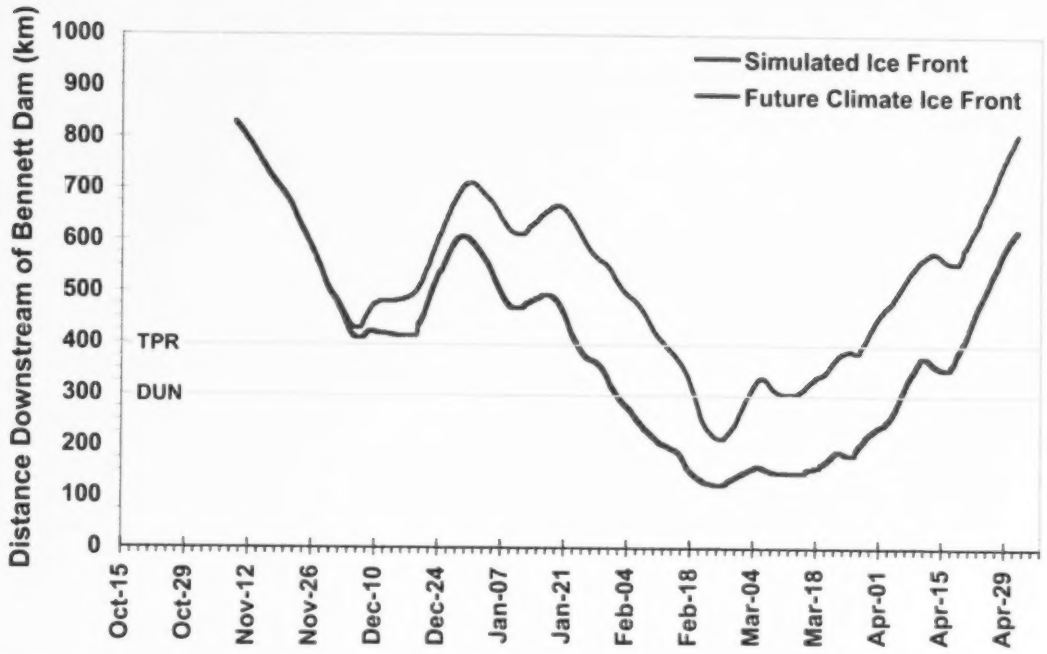

Figure B-19 Historical versus climate change modeled ice front profile – 1985/86

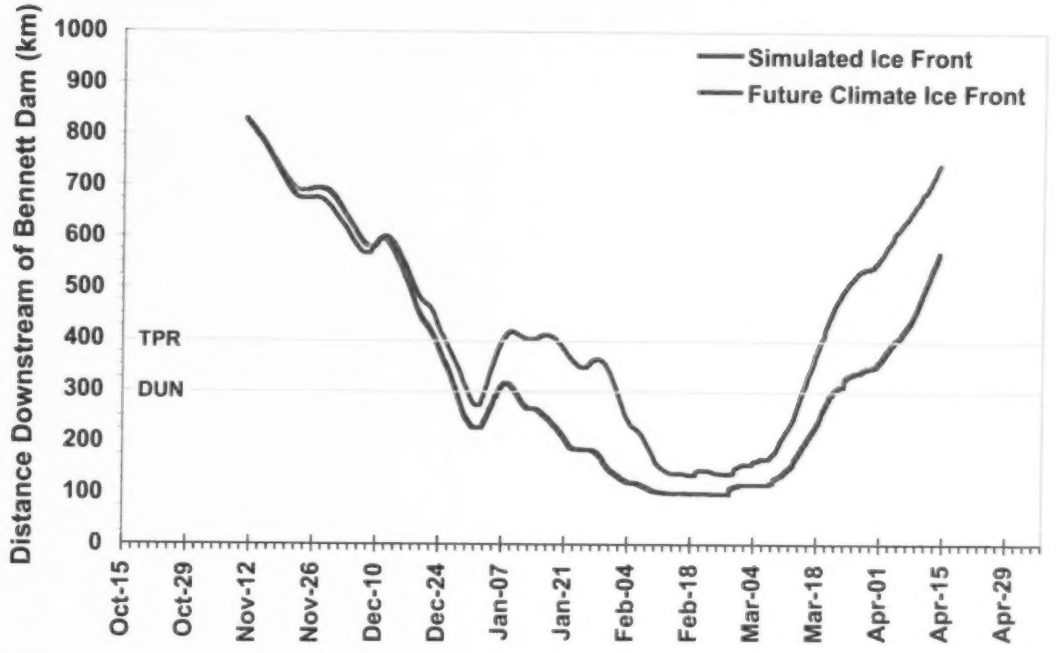

Figure B-20 Historical versus climate change modeled ice front profile – 1984/85

APPENDIX C

A2 Climate Change Scenario Storyline

An excerpt from the Intergovernmental Panel on Climate Change (IPCC)
Special Report on Emissions Scenarios (SRES) – available online:

http://www.grida.no/climate/ipcc/emission/089.htm

A2 Storyline and Scenario Family

The A2 scenario family represents a differentiated world. Compared to the A1 storyline it is characterized by lower trade flows, relatively slow capital stock turnover, and slower technological change. The A2 world "consolidates" into a series of economic regions. Self-reliance in terms of resources and less emphasis on economic, social, and cultural interactions between regions are characteristic for this future. Economic growth is uneven and the income gap between now-industrialized and developing parts of the world does not narrow, unlike in the A1 and B1 scenario families.

The A2 world has less international cooperation than the A1 or B1 worlds. People, ideas, and capital are less mobile so that technology diffuses more slowly than in the other scenario families. International disparities in productivity, and hence income per capita, are largely maintained or increased in absolute terms. With the emphasis on family and community life, fertility rates decline relatively slowly, which makes the A2 population the largest among the storylines (15 billion by 2100). Global average per capita income in A2 is low relative to other storylines (especially A1 and B1), reaching about US$7200 per capita by 2050 and US$16,000 in 2100. By 2100 the global GDP reaches about US$250 trillion. Technological change in the A2 scenario world is also more heterogeneous than that in A1. It is more rapid than average in some regions and slower in others, as industry adjusts to local resource endowments, culture, and education levels. Regions with abundant energy and mineral resources evolve more resource-intensive economies, while those poor in resources place a very high priority on minimizing import dependence through technological innovation to improve resource efficiency and make use of substitute inputs. The fuel mix in different regions is determined primarily by resource availability. High-income but resource-poor regions shift toward advanced post-fossil technologies (renewables or nuclear), while low-income resource-rich regions generally rely on older fossil technologies. Final energy intensities in A2 decline with a pace of 0.5 to 0.7% per year.

In the A2 world, social and political structures diversify; some regions move toward stronger welfare systems and reduced income inequality, while others move toward "leaner" government and more heterogeneous income distributions. With substantial food requirements, agricultural productivity in the A2 world is one of the main focus areas for innovation and research, development, and deployment (RD&D) efforts, and environmental concerns. Initial high levels of soil erosion and water pollution are eventually eased through the local development of more sustainable high-yield agriculture. Although attention is given to potential local and regional environmental damage, it is not uniform across regions. Global environmental concerns are relatively weak, although attempts are made to bring regional and local pollution under control and to maintain environmental amenities.

As in other SRES storylines, the intention in this storyline is not to imply that the underlying dynamics of A2 are either good or bad. The literature suggests that such a world could have many positive aspects from the current perspective, such as the increasing tendency toward cultural pluralism with mutual acceptance of diversity and fundamental differences. Various scenarios from the literature may be grouped under this scenario family. For example, "New Empires" by Schwartz (1991) is an example of a society in which most nations protect their

threatened cultural identities. Some regions might achieve relative stability while others suffer under civil disorders (Schwartz, 1996). In "European Renaissance" (de Jong and Zalm, 1991; CPB, 1992), economic growth slows down because of a strengthening of protectionist trade blocks. In "Imperial Harmonization" (Lawrence et al., 1997), major economic blocs impose standards and regulations on smaller countries. The Shell scenario "Global Mercantilism" (1989, see Schwartz, 1991) explores the possibility of regional spheres of influence, whereas "Barricades" (Shell, 1993) reflects resistance to globalization and liberalization of markets. Noting the tensions that arise as societies adopt western technology without western culture, Huntington (1996) suggests that conflicts between civilizations rather than globalizing economies may determine the geo-political future of the world.

References

CPB (Bureau for Economic Policy Analysis). (1992). "Scanning the Future: A Long-Term Study of the World Economy 1990-2015". Sdu Publishers, The Hague.

De Jong, A. and Zalm, G. (1991). "Scanning the Future: A Long-Term Scenario Study of the World Economy 1990-2015". In Long-term Prospects of the World Economy, OECD, Paris, 27-74.

Huntington, S.P. (1996). "The Clash of Civilizations and the Remaking of World Order". Simon and Schuster, New York, NY.

Lawrence, R.Z., Bressand, A. and Ito, T. (1997). "A Vision for the World Economy - Openness, Diversity, and Cohesion". The Brookings Institution, Washington, DC.

Schwartz, P. (1991). "The Art of the Longview: Three Global Scenarios to 2005". Doubleday Publications, New York, NY.

Schwartz, P. (1996). "The New World Disorder". WIRED Special Edition 1.10. (See also: Global Business Network. (http://www.gbn.org/scenarios).

Shell. (1993). "Global Scenarios 1992-2020". PL-93-S-04, Group Planning, Shell International, London.